The Precision Tracker

By J. V. ANDERS, E. F. HIGGINS, JR., J. L. MURRAY and F. J. SCHAEFER, JR.

(Manuscript received February 25, 1963)

The precision tracker, a simultaneous lobing, amplitude-comparison, passive, continuous-wave tracker based in principle and design upon a monopulse tracking radar, is employed at the Andover, Maine, and Pleumeur-Bodou, France, stations to find the satellite and direct the horn-reflector antennas when required and, at regular intervals during subsequent passes, to provide the precise tracking data required for prediction of future orbital parameters.

I. INTRODUCTION

The Telstar satellite radiates a 4079.73-mc continuous-wave (CW) carrier 90 mc below the frequency of the communications carrier.[1] This signal is designed as a beacon for the processes of tracking and initial acquisition. The design of the precision tracker receiver is thus based on the characteristics of this beacon signal as modified by the dynamic orbital parameters: these are listed briefly in Table I.

The system application — the manner in which the tracker is integrated into the Telstar ground system operations — is described in Ref. 2. Section II of this paper is a brief description of the precision tracker system; sections III through IX cover the several subsystems in greater detail.

II. SYSTEM DESCRIPTION

The precision tracker (hereafter referred to as the PT) is essentially a radio theodolite. From the viewpoint of the over-all Telstar system, it has one simply defined task: to provide the antenna pointing system with the real-time, locally referenced azimuth and elevation angles of the satellite.

TABLE I — NOMINAL DESIGN CHARACTERISTICS OF THE BEACON AND ORBIT

Apogee	3000 nm
Perigee	600 nm
Inclination	45 deg
Tangential velocity	302 nm/min
Beacon frequency	4079.73 mc
Doppler rate, maximum	575 cps[2]
Doppler shift, maximum	±65 kc
Precision	±4 kc
Stability	±12 kc/day
Thermal variation	±40 kc
Effective radiated power	+13 dbm

2.1 *Data Take-Off*

To provide the required angle data, the PT antenna rotates in two axes — azimuth and elevation. A multispeed gear box is associated with each axis; mechanical angle is converted by precision 1-speed and 64-speed resolvers to ac analog voltage, which in turn is converted to pulse time modulation for transmission to the track digital control unit of the antenna pointing system.

2.2 *Automatic Tracking*

The PT is a *simultaneous lobing, amplitude-comparison, passive, CW* tracker. The antenna, with its four-horn feed system, the microwave comparator, and the three-channel tracking receiver, develops output voltages proportional to the azimuth pointing error and the elevation pointing error. These error signals are passed through equalizers, modulators, and amplifiers to the azimuth and elevation drive motors, thus closing two servo loops that continuously serve to minimize the angular errors between the antenna's boresight axis and the line-of-sight to the satellite.

2.3 *Simultaneous Lobing — Amplitude Comparison*

The microwave energy received by the four feedhorns is processed by the comparator to develop three different antenna pattern response characteristics: the *sum* pattern, corresponding to a conventional antenna pattern; the *elevation difference* pattern, having two main lobes in the elevation plane with a deep null on the boresight axis; and the *azimuth difference* pattern, having two main lobes in a plane perpendicular to the elevation plane with a deep null on the boresight axis. (Strictly

speaking, this should be called the traverse difference pattern; however, the error signal is applied to the azimuth axis of the mount.)

The difference signals are developed in the comparator by amplitude summations in hybrids. The system is phase-sensitive in that the phase of the error signals relative to the phase of the sum signal is employed as an indication of the sense of the error signals, i.e., left-right and up-down.

The three-channel tracking receiver employs two stages of conversion to bring the sum, azimuth, and elevation signals down to 5 mc prior to demodulation. An AGC voltage is developed from the sum channel and applied to all three channels; thus, the demodulator outputs are proportional to D/S, the difference pattern response divided by the sum pattern response. This has two important effects. First, the angle-error function is linearized with respect to off-axis angle: the two-lobe difference pattern function is converted to a nearly linear function. Second, the output scale factor is rendered insensitive to changes in absolute received signal level within the frequency response of the AGC system and the dynamic range of the receiver.

2.4 *Signal-to-Noise Ratio*

A high probability of detection with a low false-alarm rate is required for the acquisition process; a low standard deviation in tracking error is required by the orbital prediction program. These two requirements imply certain minimum signal-to-noise objectives.

Both the tracking noise (jitter) and bias vary in a complex way with the signal-to-noise ratio (SNR) available to the signal processing circuits. Generally the bias decreases with increased SNR, while tracking jitter increases rapidly as the SNR decreases below values of about +3 db at the intermediate frequency output. The available satellite beacon power, the space transmission path, the receiver "front end" design, and the signal-processing equipment all affect the degree to which these objectives are met. The deviation in the radiation pattern of the satellite from isotropic results in variation of about 5 db; the changes in its beacon power due to communication loading result in about 2 db variation. The transmission path length change is the most significant variable, accounting for about 12 db variation over the portion of the orbit tracked. As a result, the dynamic range of input signals is expected to be in the order of 20 db, a relatively small range. Since the SNR and tracking properties vary with path length, the slant path at apogee (about 5700 statute miles) sets the most stringent requirements.

Because orbital tracking requires the tracking antenna to be directed through a wide variety of space regions, the effects of noise sources, both spot and distributed, also contribute to the over-all received signal. The sun, which could contribute some 1500°K additional to the receiver temperature if it were viewed directly, is an example of a potent spot noise source; but the most important noise source in the field of view of the system is the atmosphere. At the receiver frequency of 4079.73 mc, the atmospheric noise contribution for the PT receiver can vary from about 14°K at the zenith to 170°K at the horizon, increasing rapidly for angles below 5 degrees. Normally the system operates over elevation angles of from 7.5 to 82.5 degrees and thus never experiences the maximum noise and SNR degradation condition except during test operations.

The loss effects for the 5700-statute-mile path, including an antenna polarization loss factor, are tabulated in Table II at a reference elevation angle of 10 degrees.

A practical optimum in system noise reduction at the front end of the receiver is attained through the use of room-temperature parametric amplifiers, located in the moving antenna support structure along with the first converters and the 60-mc IF preamplifiers. The resulting system operating noise temperature (about 340° K) and received signal level (as low as −138 dbm) place severe requirements on the signal detection schemes.

2.5 *Acquisition Receiver*

The PT was designed for rapid acquisition after a few spacecraft orbits. The maximum expected uncertainties in time, angles, and frequency were used as boundary conditions for design.

Enhancement of signal-to-noise ratio by a narrow-bandwidth filter was defeated, for the initial-orbit acquisition process, by *time*: to the

TABLE II — LOSSES

Loss Type	Loss Value (db)
Divergence (path loss)	184.20
Oxygen	0.25
Water vapor	0.15
Ozone and other particles	0.10
Polarization loss, vertically polarized antenna, nearly circularly polarized signal (includes axial ratio effects)	3.00
Total	187.70

finite time required to search the volume of space expected to contain the satellite must be added, for each beamwidth increment, the time per beamwidth necessary to sweep a narrow filter across the frequency band within which the beacon frequency will lie. It was not possible to develop an efficient and simple search strategy in which the necessary search time was compatible with the rate of motion of the search volume. The solution employed in the PT is to reduce the frequency-search time essentially to zero by a stationary search conducted with a comb filter.

The equipment associated with the comb filter has been designated the acquisition receiver. As may be seen from the block diagram (Fig. 1), the acquisition receiver serves as an initial tuning control to preset the frequency of the narrow band tracking receiver. Upon sensing the presence of a signal in the sum channel, it also stops the antenna's angular search at the point where the signal was detected. Thus, at the expense of 300 channels of signal processing, the frequency-search time per unit beamwidth has been reduced from 30 seconds to the $\frac{1}{4}$-second response time of the acquisition receiver's post-detection filters and threshold detectors.

The acquisition receiver was used to advantage on July 10, 1962, at 7:25 p.m. when it set the PT to a condition of fully automatic tracking within 6 seconds after the satellite repeater had been ordered to turn on.

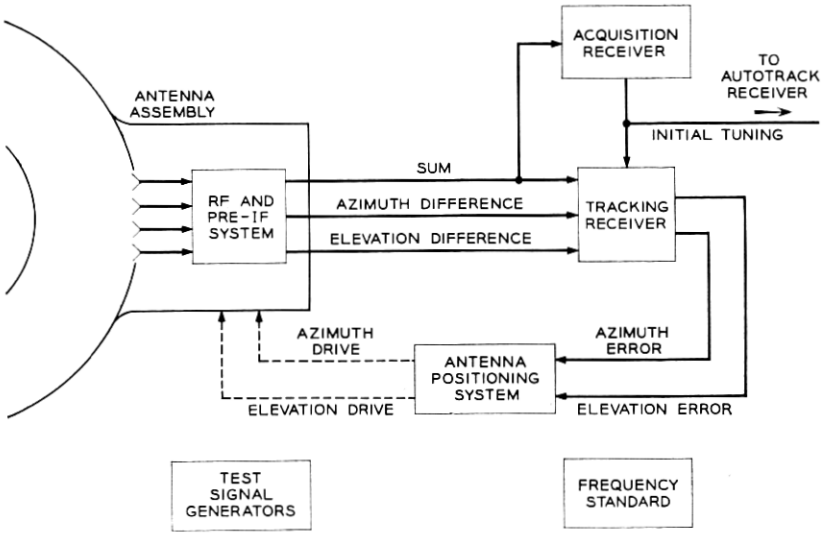

Fig. 1 — Precision tracker, block diagram.

2.6 *Tracking Receiver*

In the tracking receiver, which can develop usable angle-error signals with a signal-to-noise ratio 10 db or more below signal detection threshold, the need for maximizing the signal-to-noise ratio is based on reducing tracking jitter to the levels required by the orbital prediction program. It is also necessary to hold the jitter to levels which will damage neither the horn-reflector antenna and its associated electronic equipment nor the operating personnel when the horn-reflector is slaved to the PT. Since it is essential to recover the phase of the error signals relative to the phase of the sum signal, the demodulation technique offering the greatest noise rejection is coherent detection. The sum signal is kept in phase coherence with a noise-free 5-mc reference by a phase-lock loop or tracking filter discussed in Section IV. The 59.98-mc azimuth difference and elevation difference IF signals are converted to 5 mc by the 64.98-mc local oscillator signal developed in the phase-lock loop; thus, all three channels are maintained in phase coherence with the 5-mc reference, and coherent detection is effected in the angle error and AGC demodulators.

As a test option, the demodulation scheme may be converted to correlation detection for tracking the sun or other sources of wideband, random-phase radiation. To effect this conversion, the 5-mc demodulating reference is replaced by the 5-mc sum signal.

Under normal tracking conditions, when the tracking receiver is employing coherent detection with the phase-lock loop locked to a received CW signal with less than ± 10 degrees of phase jitter, the angular tracking jitter of the antenna is controlled by the bandlimiting effect of the servo system upon the effective receiver noise power. The nominal one-sided servo bandwidth varies from 0.2 cps to 1 cps under control of the received signal level. Thus, the narrower bandwidth reduces tracking jitter when the satellite is at longer range and the signal is weaker; the wider bandwidth reduces acceleration lag at shorter ranges where the signal is strong but the angular velocity and acceleration are greater.

The salient characteristics of the PT are listed in Table III. The following sections will describe the various subsystems of the PT in greater detail.

III. ANTENNA, RF PROCESSING, AND PREAMPLIFIERS

3.1 *Introduction*

The RF system used in the PT is composed of a low-noise antenna and comparator,[3] a high-gain, low-noise parametric amplifier, and a

TABLE III — SALIENT PARAMETERS OF THE PRECISION TRACKER

Effective receiver input temperature	315°K
Equivalent noise power in 3-kc bandwidth	−139 dbm
Received signal power at feedhorns for range of 5700 statute miles, satellite beacon power +13 dbm, PT line-of-sight to satellite's equator	−137 dbm
Received signal power at feedhorns for range of 5700 statute miles, satellite beacon power +13 dbm, PT line-of-sight 40 degrees off satellite's equator	−142 dbm
Over-all mechanical precision of antenna assembly, azimuth and elevation (1 sigma), including effects of wind loading and thermal variation on both antenna and boresight tower	0.005 deg
Tracking jitter, azimuth and elevation — standard deviation objective	0.015 deg
Slew rates	45 deg/sec
Servo bandwidth, autotracking mode	0.2, 0.5, and 1.0 cps
Acquisition time	
Angle search	0–24 sec
Acquisition receiver response	0.25 sec
Tracking receiver preset	0.45 sec
Tracking receiver frequency search	0–4 sec
Most probable time lapse from signal presence to autotrack	2.7 sec

well matched mixer-preamplifier transmission system. (See the block diagram in Fig. 2 and associated Table IV.) This arrangement ensures an adequately low receiver noise contribution.

3.2 *Antenna*

The 8-foot Cassegrainian reflector, shown in Fig. 3, provides a 2-degree beamwidth, which represents a nearly optimum compromise between the wide beam needed for acquisition and the antenna gain required for tracking accuracy. The antenna system is a unique embodiment of the Cassegrainian configuration; it consists of a parabolic main reflector, a hyperbolic subreflector, and a four-horn feed system which illuminates the subreflector from the rear through a hole at the axis of the main reflector. It is designed to process an impinging wave front polarized vertically. For any other polarization it may be considered as accepting only the vertical vector component; thus, for the nominally circularly polarized Telstar spacecraft beacon signal, a 3-db effective loss is entailed.

3.2.1 *Reflector Assembly*

Fiberglas honeycomb is the main structural material employed in the reflector assembly, as shown in Fig. 3. The subreflector and its conical support constitute an integral structure of molded Fiberglas honeycomb core overlaid on both sides with a Fiberglas skin. The conducting hyper-

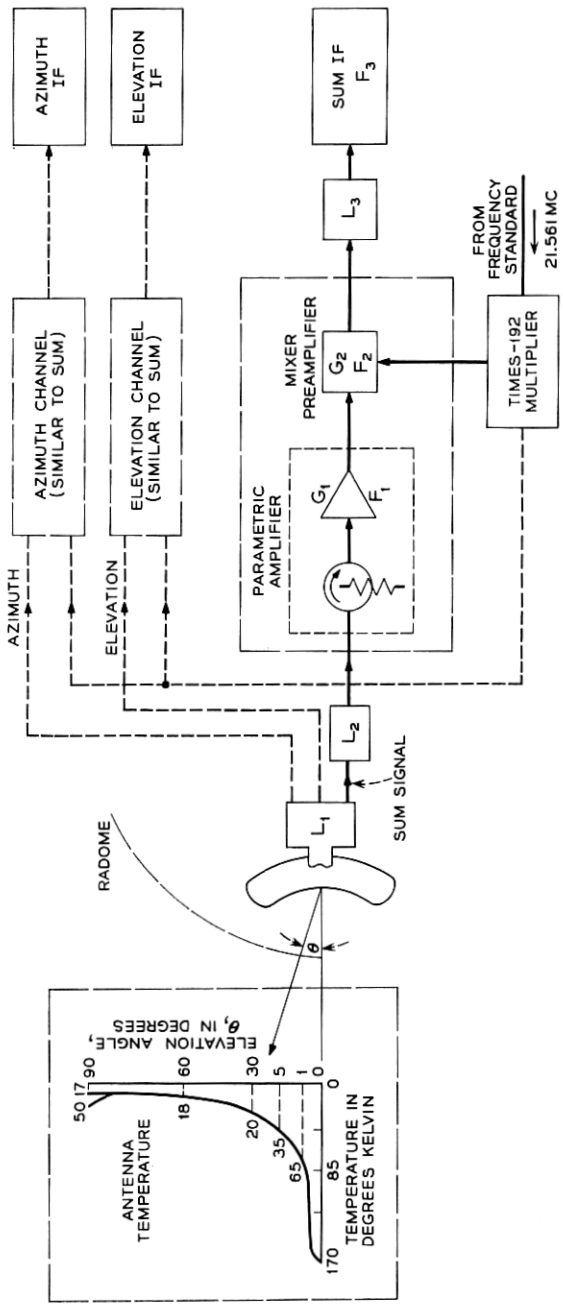

Fig. 2 — Over-all RF block diagram.

TABLE IV

Antenna and Radome Temperature	Comparator Loss	Coupling Losses, Semi-Rigid Line	Parametric Amplifier, Mixer-Preamplifier and Harmonic Multiplier	Slip Rings and Coax Cables	Main IF Amplifier
Radome $\approx 9°K$ System input temperature (T_e) $T_e = \sum_{1}^{n} \frac{(T_a)n}{\prod_{n}^{(1-n)} G(n-1)} = 315°K$ System operating temperature (T_{op}) $T_{op} = T_{ant} + T_e$ $= 340°K$ at $\Theta = 10°$	Dissipative and mismatch loss $L_1 \approx 0.2$ db $T \approx 290°K$ Connector loss = 0.1 db Total $L_1 = 0.3$ db	Rigid cable loss at 4079.73 mc $L_2 = 0.2$ db	Over-all unit noise figure 2.7 db Circulator loss 0.2 db $G_1 = 23$ db, including circulator $G_2 = 25$ db $F_1 = 2.5$ db $F_2 = 9$ db max.	Ring loss 0.4 db Cable loss 4.2 db Connectors 0.2 db Total 4.8 db	$F_3 = 9$ db $T = 290°K$

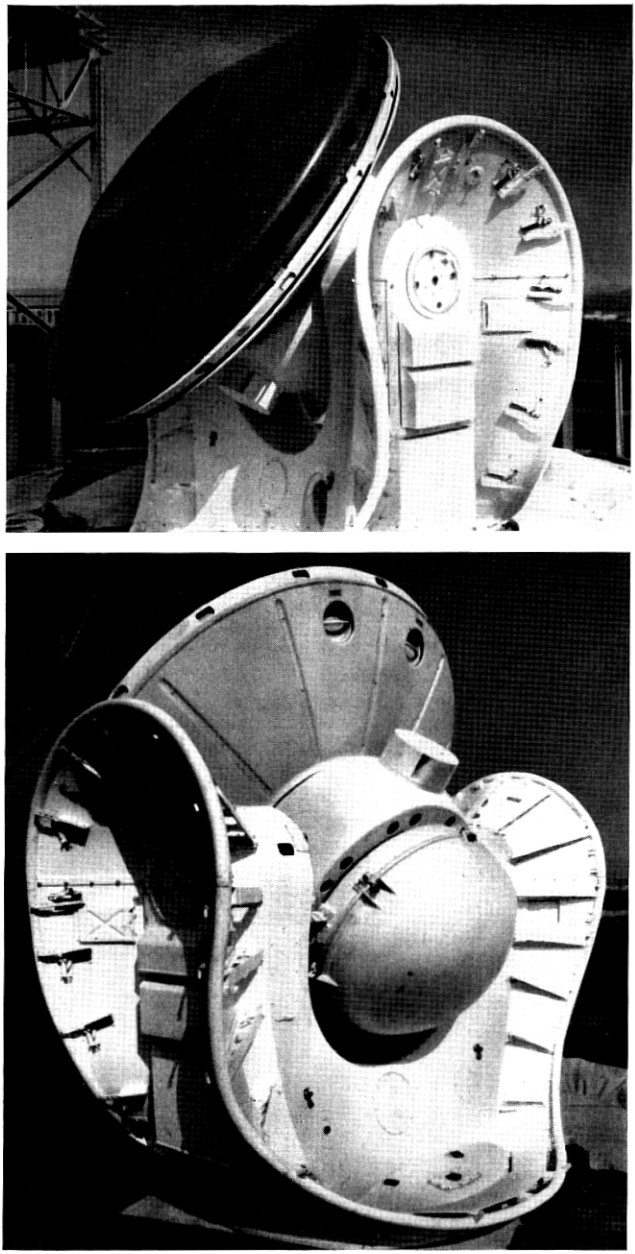

Fig. 3 — Precision tracker antenna, front and rear views.

bolic surface of the 36-inch diameter subreflector is composed of a horizontal array of aluminum wires of 0.01-inch diameter embedded in both the inner and outer skins. The subreflector is transparent to impinging vertically polarized signal components (see Fig. 4). The periphery of the area containing the wires is serrated rather than circular, to cause cancellation of the major effects of diffraction at the wire ends. The subreflector is 26.6 inches in front of the main reflector along the boresight axis.

The 92-inch diameter main reflector is made up of an aluminum parabolic reflector surface on which is overlaid a Fiberglas honeycomb core. The Fiberglas skin affixed to the core contains an aluminum wire grid embedded at an angle of 45 degrees to the vertical. The structure is called a twist-reflector: a vertically polarized signal component impinging upon the surface of the 45-degree wires may be resolved into two vector components, one normal to the wires and the other parallel to the wires. The parallel component is reflected by the wires; the normal component passes through the wires and honeycomb core and is reflected from the aluminum reflector to pass back through the core and the wires. The delay through the core is such that the two components recombine, at the wire surface after reflection, to result in a horizontally polarized signal at the subreflector.

The subreflector, whose wire structure is opaque to horizontal polarization, refocuses the signal to the four feedhorns projecting through the center of the main reflector.

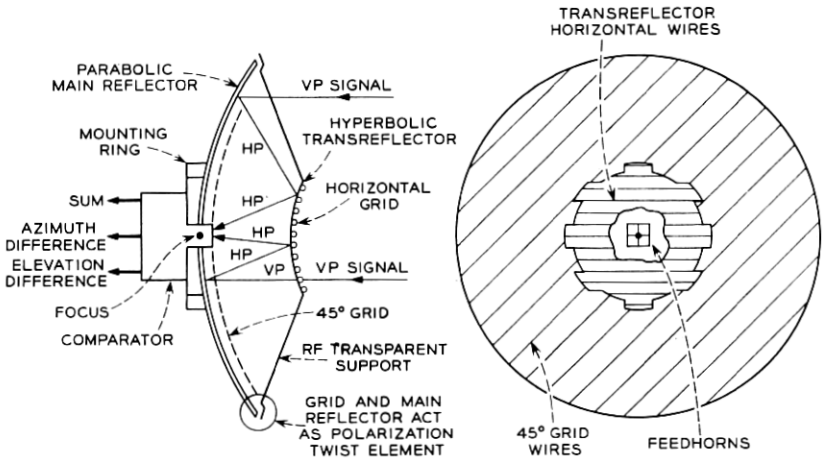

Fig. 4 — Cassegrainian antenna and twist reflector.

3.2.2 *Comparator-Feed Assembly*

Four individual patterns, each "squinted" symmetrically away from the central boresight axis of the antenna system, are created by the four horns and reflectors. The feedhorns are an integral part of the comparator-feed assembly, illustrated in Fig. 5, which shows the assembly, the microwave absorber ring which surrounds the feed, and the Fiberglas dust cover.

The assembly is made from aluminum stock in which the horns, four waveguide hybrid junctions, and waveguide phasing sections are precisely machined. The signals received by the horns are processed by vector additions and subtractions in the hybrids to form the three antenna response functions[4] required for tracking. The sum pattern is formed by the summation of all signals propagating in the four horns; the azimuth difference and elevation difference patterns are formed by obtaining the difference between the sums of signals in adjacent vertical pairs and horizontal pairs, respectively.

Connections from the signal output ports of the comparator to the parametric amplifiers are made by waveguide-to-coaxial transitions and through semirigid, low-loss coaxial line.

3.2.3 *Advantages of the Antenna System*

The Cassegrainian antenna as employed in the PT has the following advantages:

(a) It possesses the high gain associated with parabolic structures.

(b) Secondary radiation patterns having excellent sum pattern symmetry and difference patterns with high slope factors and deep boresight nulls are achieved.

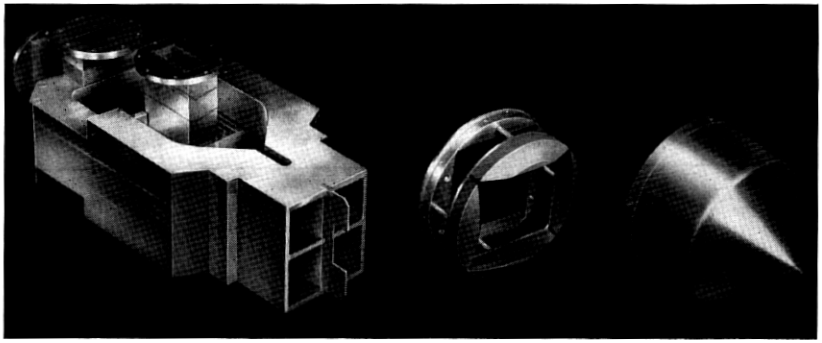

Fig. 5 — Microwave comparator (photo courtesy Wheeler Laboratories, Inc.).

(c) Shadow effects are minimized by the subreflector design, and therefore the effective area is essentially the same as that of an equivalent-sized parabolic system.

(d) Since the focal point is in the parabolic contour, the comparator can be located near the RF amplifier, thus minimizing coupling loss noise; the effective receiver temperature is lowered over that of antenna-receiver types having forward feeds and feed-support schemes.

(e) Since tracking angles are above the horizon, the primary patterns are coupled to the low-temperature sky rather than to the high-temperature earth; therefore, the effect of increased noise due to the primary radiation pattern coupling is lessened.

(f) Side lobes, back radiation, and spillover lobes are well below peak response (see Fig. 6 and associated Table V).

(g) A structure of relatively low moment of inertia is obtained, since the heavy receiving components are located near the rotational axis.

3.3 *Parametric Amplifiers*

Three low-noise parametric amplifiers amplify the sum and difference signals prior to mixing. These amplifiers are of the nondegenerative negative-resistance type. The input signal is fed through an input circulator, an impedance transformer, and a low-pass filter, so as to match the impedance at the varactor element and minimize coupling between the idler, pump, and signal circuits. The varactor element is mounted in a cavity resonant at both the pump frequency (16 kmc) and the idler frequency (12 kmc). The pump signal is produced by a reflex klystron which is immersed in a temperature-controlled oil bath and coupled to the parametric amplifier via K-band waveguide sections. The specifications for the PT parametric amplifiers are given in Table VI.

The parametric amplifier outputs for the three channels are fed to a balanced mixer-preamplifier unit. These units have an over-all gain of 25 db and a maximum noise figure of 9.0 db (double channel). The preamplifier utilizes a cascade circuit to minimize the over-all noise figure of the mixer-preamplifier assembly. The preamplifier has a center frequency of 59.98 mc and a bandwidth, at a -3 db response, of 6 mc.

Local oscillator drive is supplied to all three mixers by a common solid-state harmonic multiplier. This unit produces a minimum of 3 mw of RF power for each mixer at a frequency above the signal input. The output signals from the preamplifier are matched to 50-ohm coaxial cables and supplied to the slip rings for transmission from the rotating portion of the antenna assembly to the stationary tracking mount.

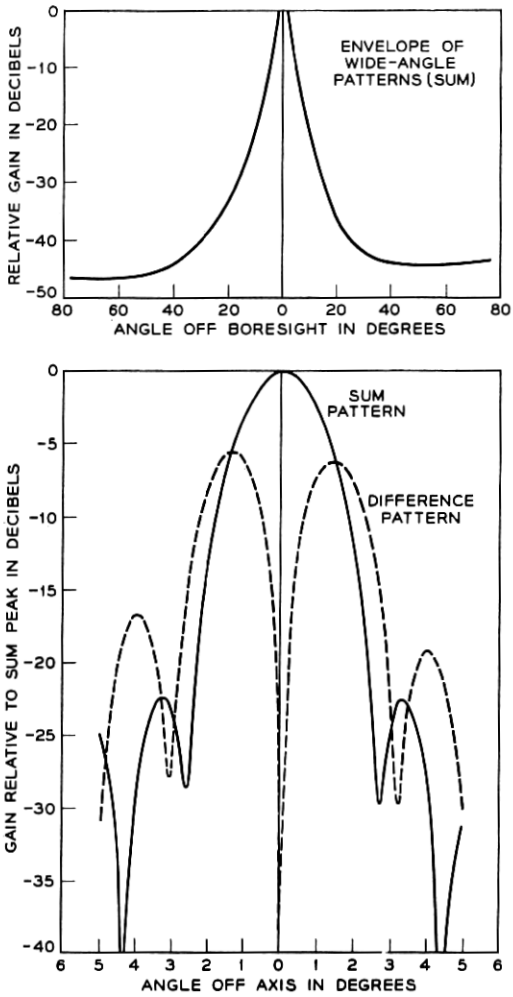

Fig. 6 — Secondary radiation pattern of precision tracker antenna system.

TABLE V — NOTES FOR FIG. 6

Antenna Characteristic	Value
Frequency	4079.73 mc
Polarization	vertical
Sum gain	37.2 db
3-db beamwidth, sum mode	2.1°
Suppression of first side lobe, sum mode	22.3 db
Difference gain, average of EL and AZ	30.6 db
Difference peak separation, average of EL and AZ difference modes	2.8°
Suppression of first difference side lobe, average of EL and AZ difference modes	12.6 db
Difference slope, normalized to an isotropic radiator	43.5v ratio/deg.

TABLE VI — PARAMETRIC AMPLIFIERS

Parameter	Value
Center frequency	4079.73 mc
Gain	23 db nominal
Bandwidth, instantaneous	20 mc nominal
Pump frequency	16,037 ± 2 mc
Pump power	60 mw nominal
Noise figure, excluding coupling losses	2.5 db max.
Gain stability, channel to channel	3 db max. fluctuation
Phase stability, channel to channel	12° max. fluctuation

The 50-ohm coaxial preamplifier lines are matched to the rings by a shorted stub element attached to each of the three signal rings. A 50-ohm double-shielded coaxial cable transmits the IF signals to the main IF amplifier.

3.4 *Signal-to-Noise Ratio*

A determination can be made of the SNR achieved for the system, taking into account the added noise components due to the atmosphere and the properties of the receiver components. The noise producing elements are defined as those up through and including the slip-ring assembly (see the block diagram of the RF system, Fig. 2, and associated Table IV). The receiver's effective input temperature, obtained from the component values shown here, is determined to be 315°K. Adding the antenna temperature to this value gives the system effective operating noise temperature (T_{op}). The effective input noise power ($P_n = KT_{op}B$) can then be obtained for each elevation angle. The results are shown in Fig. 7, together with the expected received signal power (P_s) for the 5700-statute-mile path. The SNR is the difference in ordinates between the two functions. It can be seen that the receiver and antenna noise contribution over the operational range of angles reduces the SNR value, based on the noise power associated with an input termination in thermal contribution over the operational range of angles reduces the SNR value, equilibrium at 290°K, by some 0.7 db. The average SNR over the operational elevations for maximum slant range is +3 db for a beacon signal at +15 dbm, or +5 dbm for a beacon signal power of +17 dbm.

IV. TRACKING RECEIVER

The precision tracker's tracking receiver (fifth bay of Fig. 8) functions to extract azimuth and elevation pointing error information from noise-laden IF signals produced in the tracking antenna and RF assembly by

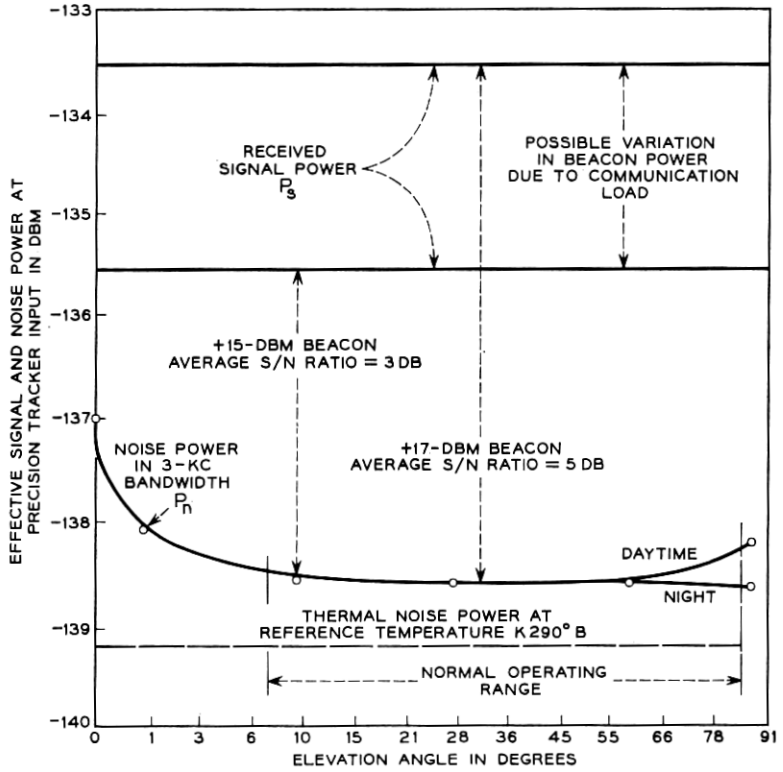

Fig. 7 — System noise power.

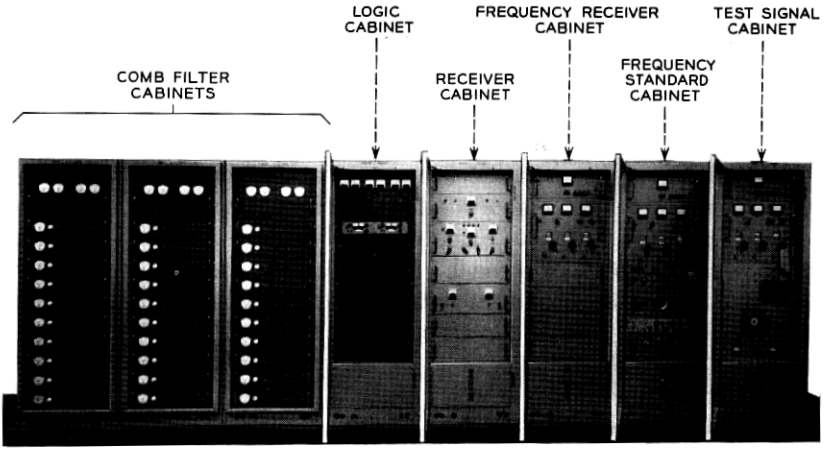

Fig. 8 — PT equipment cabinets.

a 4079.73-mc CW tracking beacon in the satellite. Because of the combined effects of Doppler shift and satellite frequency drift, the received IF signal frequency may differ from a nominal center frequency of 59.98 mc by as much as ±120 kc. A narrow-band adaptive tracking filter provides a phase-locked second local oscillator signal to permit coherent signal detection over a frequency range of ±150 kc.

4.1 *Block Diagram Description*

A simplified block diagram of the complete tracking receiver is shown in Fig. 9. The nominal 59.98-mc IF signals from the three IF preamplifiers in the antenna RF equipment enclosure are transmitted through matched slip rings and 250 feet of triple coaxial cable to the inputs of the sum, azimuth, and elevation main IF amplifiers. These matched amplifiers, under automatic gain control (AGC), provide a large portion of the 151-db receiver gain necessary to amplify the received signals to detector level. Each main IF amplifier is divided into two sections, with a bandpass filter of 1-mc bandwidth located between the sections to reduce the total noise and interference imposed on the amplifiers following.

The signal frequency is reduced to 5 mc at the three second converters by mixing with a nominal 64.98 mc derived from a voltage-controlled crystal oscillator (VCXO) and multiplier chain. The frequency and phase of this oscillator are determined by phase comparison of the 5-mc sum IF signal with a local phase-stable 5-mc reference signal in a somewhat sophisticated phase-lock loop. As shown on the block diagram, this loop also contains 5-mc IF amplifiers, a limiter, a 3-kc bandwidth crystal filter, a phase detector, and the loop filter.

The three remaining 5-mc channels are similar in that they contain 5-mc IF amplifiers, 3-kc bandwidth crystal filters, and phase detectors, all supplied by the same 5-mc reference signal. The phase-lock loop establishes and maintains a constant phase relationship between the received signals and the 5-mc reference signal, and permits coherent detection of the IF signals in these three channels. The detected sum signal provides an indication of phase lock and a measure of the received signal amplitude for operation of the AGC loop. The detected azimuth and elevation signals provide both sense and magnitude of antenna pointing errors for application to the respective antenna-positioning servos.

Biases that might occur in the pointing information because of detector unbalance or dc amplifier drift are eliminated by commutating the phase of the 5-mc IF error signals prior to detection and then synchronously demodulating the ac-coupled detector outputs.

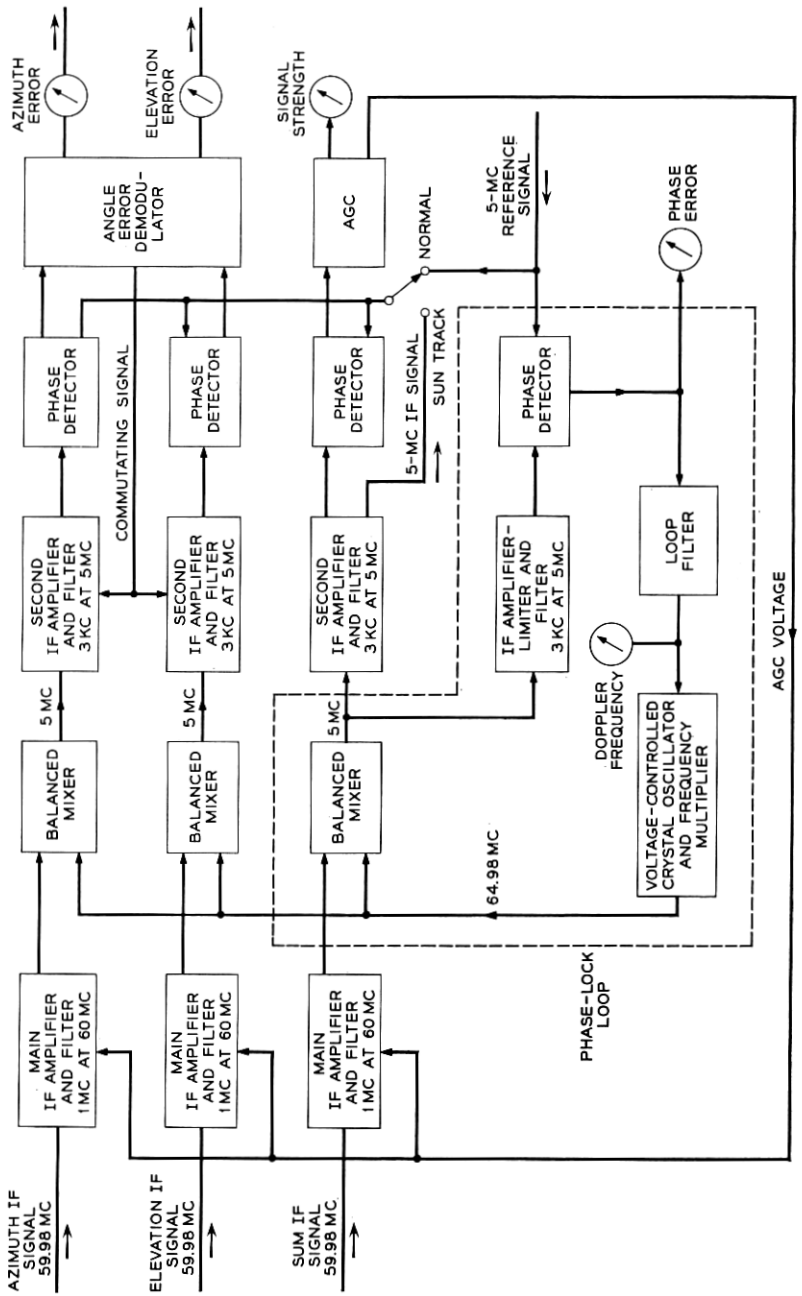

Fig. 9 — Tracking receiver, block diagram.

The mechanism for the correlation detection test option is indicated on the diagram as a "sun track" switch. The switch controls the substitution of a properly phased 5-mc sum IF signal for the 5-mc reference supplying the AGC and angle-error detectors.

A more detailed discussion of the key features of the tracking receiver follows.

4.2 *Main IF Amplifiers*

The two sections of each main IF amplifier include a total of ten transitionally coupled, synchronously tuned amplifier stages utilizing Western Electric 5847 electron tubes at a center frequency of 60 mc and an over-all bandwidth of 8 mc. The first two stages, which employ fixed gain, are followed by an adjustable phase-control network that provides approximately 150 degrees of receiver phasing adjustment per channel. The IF signal for the PT acquisition receiver is tapped off the sum channel at this point. Manual gain adjustment of the first two stages of the azimuth and elevation channels provides ±4 db of receiver gain equalization.

The remaining eight amplifier stages of each channel are gain controlled by the AGC. The stability of the amplifiers is such that the differential gain and phase of the three channels do not exceed 1 db and 3 degrees, respectively, when controlled over a 60-db range of gain from a common gain-control voltage.

A passive LC filter of 1-mc bandwidth separates the two sections of each channel for intermediate reduction of noise bandwidth.

Insertion pads are included at the input of each channel for the connection of a common IF test signal originating in the PT frequency standard and test signal cabinets.

4.3 *Second Converters*

The 59.98-mc IF signals from the three main IF amplifiers are converted to 5 mc by mixing with a common 64.98-mc local oscillator signal in three balanced passive mixers. Each input signal is terminated in a 50-ohm impedance provided by a broadband toroidal transformer hybrid. Mixing is accomplished in a matched pair of 1N35S germanium diodes.

4.4 *5-mc IF Amplifiers*

Conventional single-tuned amplifiers utilizing Western Electric 403B and 404A electron tubes follow mixer impedance matching networks

in the three channels. A 5-mc crystal lattice filter with a 3-kc noise bandwidth and a 180-degree phase delay is located, with appropriate input and output matching networks, between the first and second amplifier stages of the azimuth and elevation channels and the AGC branch of the sum channel. In the third stage of the azimuth and elevation channels, signal impedance is lowered to 50 ohms to drive a phase-commutating transformer, the operation of which will be detailed later. A fourth stage drives the 50-ohm phase-detector transformer. Following the second stage the AGC channel is split into two 50-ohm output stages, one driving the AGC detector transformer and the other providing 5-mc sum IF signals for correlation detection. The net gain of all three channels from mixer input to detector transformer is fixed at 45 db. The level of the signal appearing at all detector transformers is +13 dbm when the azimuth and elevation error signals equal the sum signal.

4.5 *Phase-Lock Loop*

The phase-lock loop is the heart of the tracking receiver. It embodies a form of adaptive tracking filter that approaches an optimum filter under all conditions of SNR, Doppler change, and rate of change expected in the PT environment.[6]

A block diagram of the phase-lock loop is shown in Fig. 10. The 5-mc IF input signal obtained from the second mixer in the sum channel is amplified approximately 75 db at a bandwidth of 200 kc by three single-tuned amplifier stages and is "hard" limited by a type 6BN6 limiter. The gain is sufficient to ensure at least 20 db of signal limiting at all times. A crystal filter with associated matching networks follows the limiter.

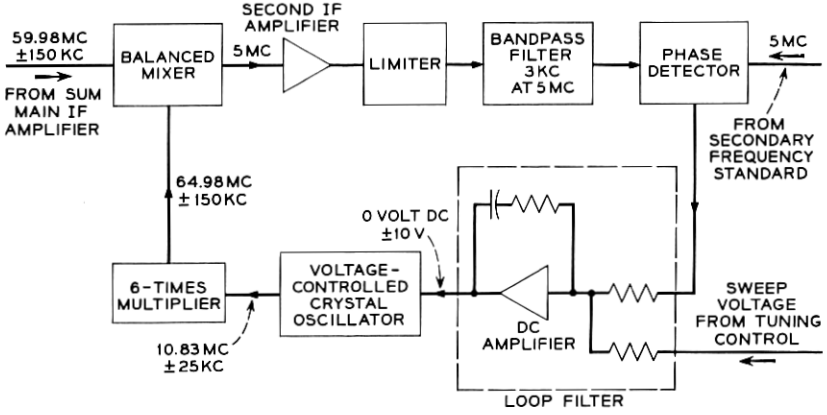

Fig. 10 — Phase-lock loop, block diagram.

This filter is similar to those in the other 5-mc IF channels in that it has a 3-kc bandwidth, but it has only a 90-degree phase delay. The requirement for a 90-degree phase difference between the reference for the phase detector in the phase-lock loop and the reference for all the other phase detectors is thus satisfied by the relative phase delays of the filters used in the 5-mc IF circuits.

A single amplifier stage matches the filter output to the 50-ohm phase-detector transformer. The signal power reaching the detector is a function of the SNR in the limiter. Because the total signal-plus-noise power in the output of the limiter is constant, the signal power at the detector will be suppressed as the direct ratio of noise-to-signal appearing at the limiter input for the ratios above approximately unity in the 200-kc bandwidth at this point. A direct consequence of this action is a reduction of phase-lock loop gain with decreasing received signal strength.

The phase detector (Fig. 11) consists of a carefully balanced and shielded broadband transformer hybrid driving a matched pair of silicon diode detectors. A high-gain dc operational amplifier accepts the two detector outputs in a differential connection to provide a low-impedance, single-ended output. Amplifier gain, and thus the phase detector gain constant, is determined by the ratio between input and feedback resistors. The 5-mc reference signal is applied to the phase detector at a much higher level than the IF signal, resulting in a sinusoidal output

$$e = \alpha K \sin \theta$$

where

α = limiter suppression factor
$K = 5.75$ = detector gain constant
θ = loop phase error.

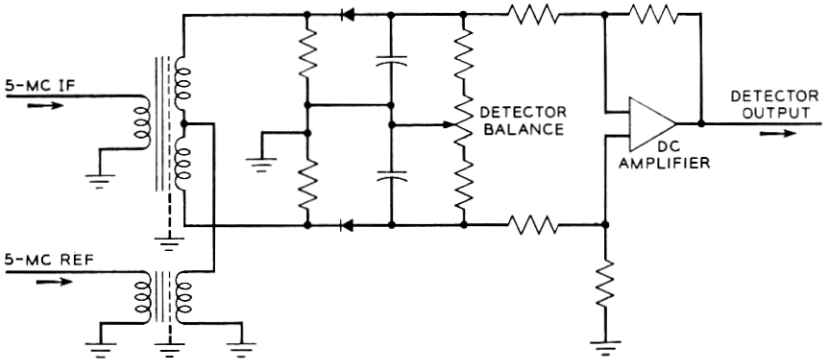

Fig. 11 — Phase detector.

The detector parameters given produce an output of 0.1 volt/degree for $\theta \leqq \pm 10$ degrees and a suppression factor of unity (strong signal).

The phase detectors of the azimuth, elevation, and AGC channels differ from this configuration only in differential amplifier gain.

The loop filter takes a form approaching that of an ideal integrator modified for loop stability. A high-gain, chopper-stabilized, dc operational amplifier with a capacitor in the feedback loop provides a dc gain of 30×10^7, falling off at 6 db/octave above 0.032 cps. This, combined with the inherent 6 db/octave slope of the VCXO/phase-detector combination, causes gain crossover to be approached at 12 db/octave. A resistor in the integrator feedback provides a lead corner at approximately 10 cps to stabilize the phase-lock loop. Because of limiter suppression, with the attendant change of loop gain, both loop bandwith and damping factor change with received SNR in a manner that optimizes the loop characteristics for minimum phase error. A plot of loop bandwidth and damping factor versus SNR is shown in Fig. 12. The use of an integrator as the loop filter results in negligible accumulated phase error at the extremes of the ± 150-kc tracking range.

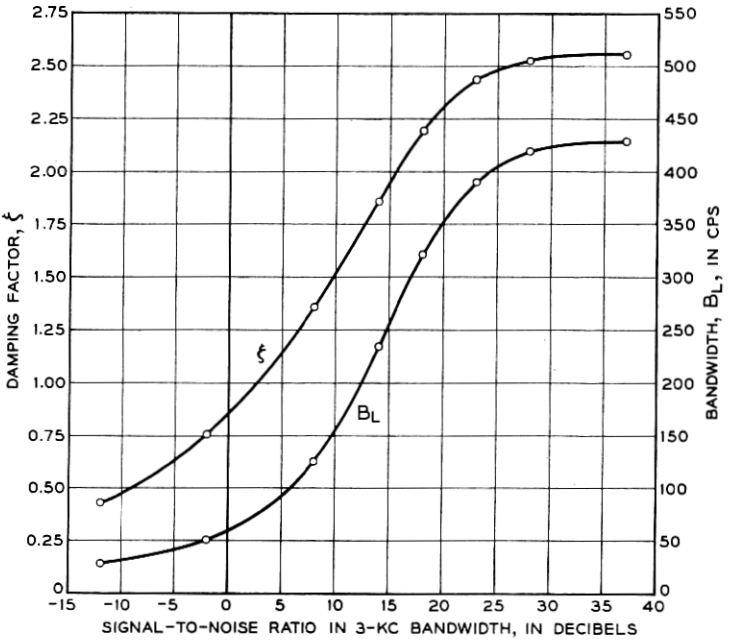

Fig. 12 — Loop bandwidth and damping factor vs signal-to-noise ratio.

During frequency acquisition the integrator is automatically preset to a voltage equivalent of 3 kc below the frequency indicated by the acquisition receiver and swept, by means of a dc voltage applied to the integrator through a separate input resistor, to the equivalent of 3 kc above indicated frequency. When phase lock occurs, the sweep is automatically disabled. The choice of one of four sweep rates is based on predicted signal strength. Manual preset and sweep controls are also provided.

The variable frequency element in the phase-lock loop is a voltage-controlled crystal oscillator (VCXO) with a stable center frequency of 10.83 mc. To permit accurate transfer of frequency acquisition information from an independent source, the voltage-frequency linearity is held to ±1 per cent of a straight line function having a slope of 2.5 kc/volt over a ±25-kc range. The unit is a commercially obtained solid-state device packaged in an oven.

The 10.83-mc (±25 kc) oscillator output is multiplied to 64.98 mc ± 150 kc by a tripler and a doubler. Three separate output stages are provided to drive the three balanced mixers at +20 dbm.

Performance of the phase-lock loop has demonstrated a capability of holding peak phase errors to a level of less than ±10 degrees over the full dynamic range of tracking conditions encountered in the PT. Good coherent detection of azimuth and elevation error signals, with the associated benefits accrued in the low SNR region, is thus assured.

4.6 *Automatic Gain Control*

Because of the phase relationships established by the crystal filters in the 5-mc IF amplifiers, the AGC phase detector provides coherent detection of the peak amplitude of the sum IF signal. The gain of the detector differential amplifier is such that a +13 dbm IF signal produces +25 volts output.

A simplified version of the AGC amplifier and loop filter is shown in Fig. 13. A dc operational amplifier, with current booster, is operated as an integrator. An adjustable limiter is provided to limit the maximum positive output voltage, thus limiting the maximum receiver gain. The +25-volt AGC detector output is compared with a nominal −25 volts in the input summing network to provide the necessary error signal for loop operation. The diodes in the capacitor feedback circuit switch an additional capacitor into the loop during signal increase to equalize loop response times for increasing and decreasing signals. Integrator time constants result in a closed-loop cutoff frequency of approximately 3 cps. Because of the extremely high dc loop gain provided by the opera-

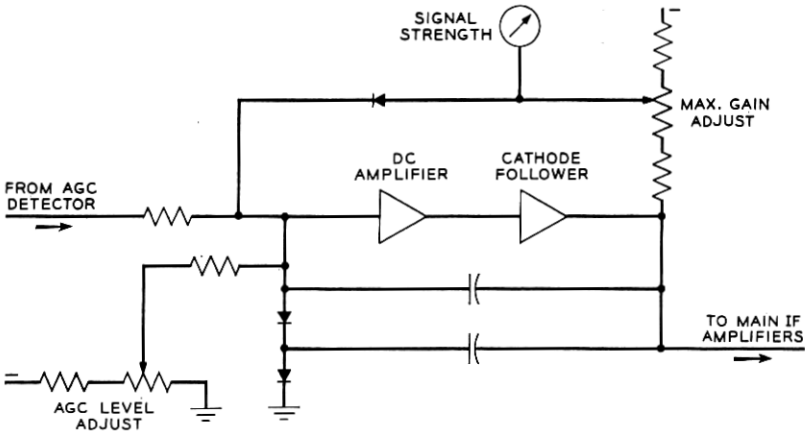

Fig. 13 — AGC amplifier and loop filter.

tional amplifier, there is negligible change in detected signal level over the entire range of gain control.

4.7 *Angle-Error Detectors*

As in the AGC detector, the azimuth and elevation phase detectors provide coherent amplitude detection of the 5-mc IF signals. The polarity of the detector output depends upon the direction of the antenna pointing error.

The prediction program, which employs the PT data, is particularly sensitive to bias errors in the angular position data obtained in the process of tracking. Bias errors of large magnitude could occur in angle-error detectors and dc circuits associated with the detectors. A commutation technique used in the tracking receiver to eliminate these errors is shown in Fig. 14. The phase of the 5-mc IF error signal is periodically reversed by the switching action of diodes in the secondary of a balanced transformer, initiated by a square wave generated at about 50 cps. As a result, the detector output becomes a square wave containing the angle error information in its amplitude. A capacitor blocks any dc bias content and couples the square wave for amplification and synchronous demodulation in a carefully balanced ring demodulator, using the same switching square wave as reference.

Detector and demodulator gain constants, together with the antenna difference pattern slope factor, result in a nominal 7.14-volt/degree pointing error scale factor at the antenna servo input. Some gain adjust-

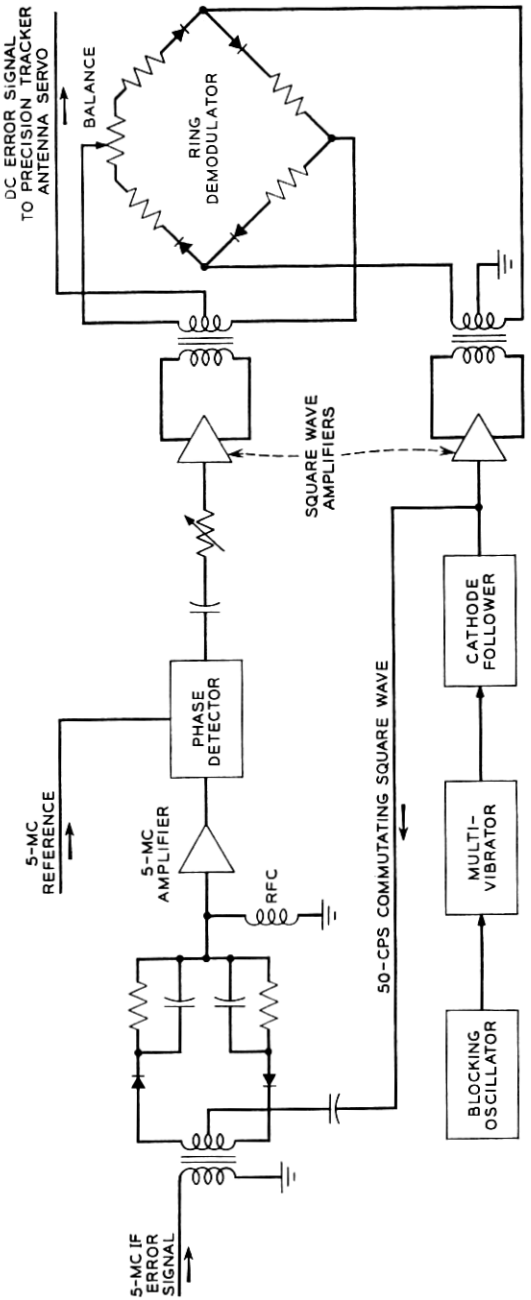

Fig. 14 — Angle-error detector commutation.

ment is provided at the demodulator input for over-all antenna servo loop gain adjustment.

V. ANTENNA POSITIONING SYSTEM

5.1 *General Description*

The antenna positioning circuits permit automatic, manual, or test control of the PT antenna. The positioning circuits consist basically of similar azimuth and elevation servo loops, which operate antenna drive motors.

In the automatic tracking mode of the precision tracker, antenna positioning data for the servo loops are in the form of azimuth and elevation error signals from the tracking receiver. Before these signals can be generated, however, the precision tracker must acquire the 4079.73-mc beacon signals from the Telstar spacecraft. To do this, input data from the track digital control or the command tracker drive the antenna positioning circuits.

During the initial stage of satellite acquisition, azimuth and elevation error signals from the track digital control point the PT antenna to the predicted position of the satellite, as described in Ref. 2. When the 4079.73-mc beacon signal is acquired by the precision tracker, the scan program is automatically stopped, the antenna positioning circuits of the precision tracker switch to the automatic tracking mode, and pointing signals from the command tracker are automatically removed.

During its acquisition and tracking operations, the precision tracker uses data on the predicted range of the satellite to optimize the frequency search rate in the tracking receiver and the bandwidths in the antenna positioning circuits. Normally, the range data are supplied in printed form by the on-site data processing system prior to the pass.

Once the 4079.73-mc beacon signal from the satellite has been acquired and the antenna positioning circuits are operating in the automatic tracking mode, the precision tracker can supply precise azimuth and elevation data to the antenna pointing system and to the data processors via the track digital control.

If because of some external or local disturbance, the precision tracker should lose autotrack, the 4079.73-mc signals may be reacquired in several ways. The precision tracker again may be slaved to the command tracker (if the CT itself is still in autotrack); the PT antenna may be repointed with predicted satellite position data from the track digital control; or the precision tracker may be placed in the manual tracking

mode. During reacquisition by any of the above means, manual or automatic scanning may be employed.

The antenna positioning circuits can be operated in any one of the following six modes:

(1) manual (test and backup acquisition mode)
(2) aided (test mode)
(3) track digital control (acquisition mode)
(4) autotrack (operational mode)
(5) command tracker (acquisition mode)
(6) remote (test and maintenance mode).

5.2 *Servo Drive Circuits*

Basically, each of the antenna positioning circuits comprises a main servo drive circuit and several servo control circuits, as shown in Fig. 15. Since the antenna positioning circuits for azimuth and elevation are electrically similar, Fig. 15 is applicable to both circuits. The main servo drive circuit is shown outlined in heavy brackets. All other circuits, outlined in light brackets, are a part of the servo control circuits.

The main servo drive circuit amplifies relatively low-level control signals to the higher power levels required to position the PT antenna mechanically. The circuit consists essentially of an input network, preamplifier, four magnetic amplifiers, four drive motors, and four tachometers.

The input network consists of three low-pass filters. One of these 0-6-0-6 db/octave filters is selected for insertion in the track loop, depending upon the range between the tracker and satellite. The widest bandwidth filter is used for the low-range, fast-moving portion of the pass, while the lowest bandwidth is used during the early, long-range portion of the pass. An additional 6-db/octave roll-off is present because of the servo closed-loop motor-tachometer combination. The 6-db/octave roll-off causes the servo to be of the velocity type 1 variety. Table VII shows a plot of open-loop gain versus frequency, and lists some of the associated parameters of the servo system.

5.3 *Manual and Aided Modes*

The manner in which the control signals are generated depends on the PT mode of operation. During either the manual or the aided mode, the control signal is generated by means of a handwheel mounted on the PT control console. During the manual mode, rotation of the handwheel generates a drive signal, which represents desired speed and direction

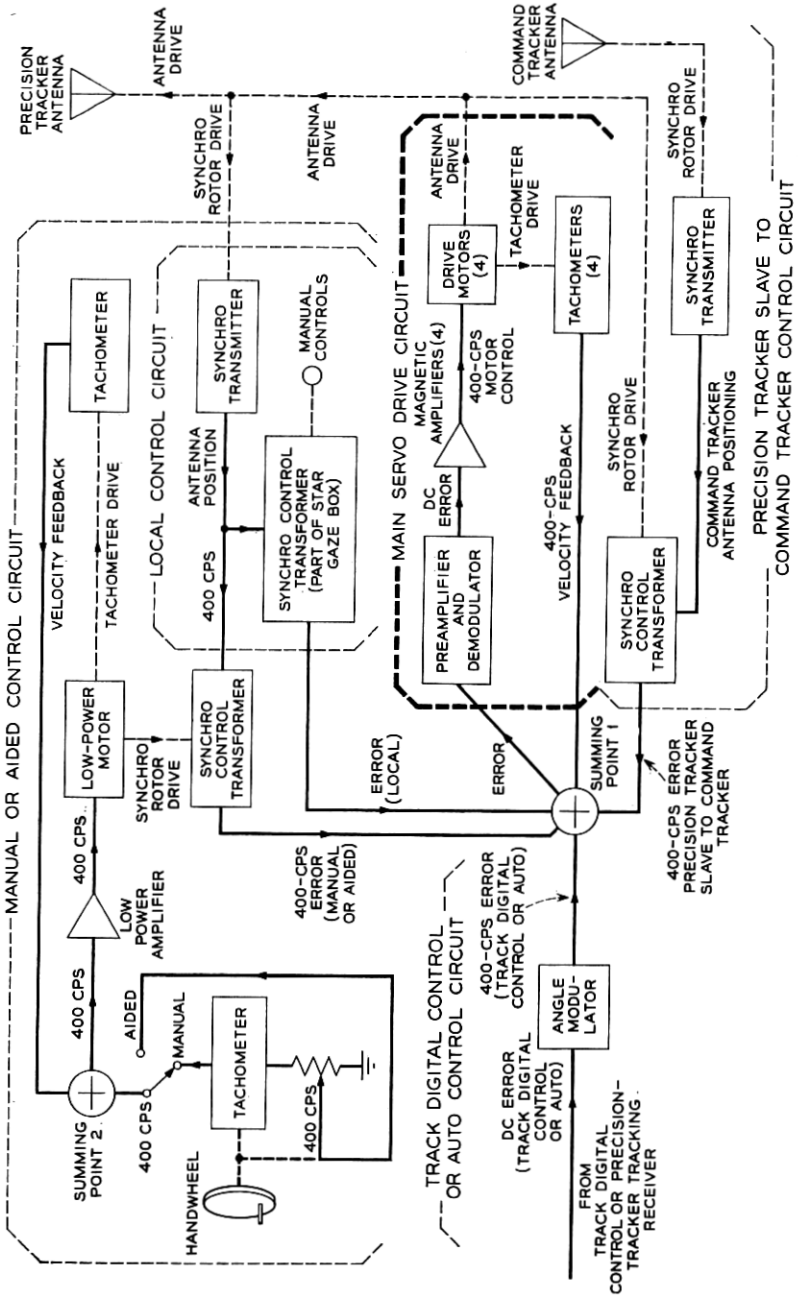

Fig. 15 — Antenna positioning circuits, azimuth or elevation.

TABLE VII — SERVO TRANSFER FUNCTION AND CONSTANTS

Open-Loop Transfer Function

$$G = \frac{\left(\frac{S}{\omega_2} + 1\right)}{\left(\frac{S}{\omega_0}\right)\left(\frac{S}{\omega_1} + 1\right)\left(\frac{S}{\omega_3} + 1\right)}$$

Closed-Loop Transfer Function

$$K = \frac{\left(\frac{S}{\omega_2} + 1\right)}{\left(\frac{S}{\omega_2} + 1\right) + \frac{S}{\omega_0}\left(\frac{S}{\omega_1} + 1\right)\left(\frac{S}{\omega_3} + 1\right)}$$

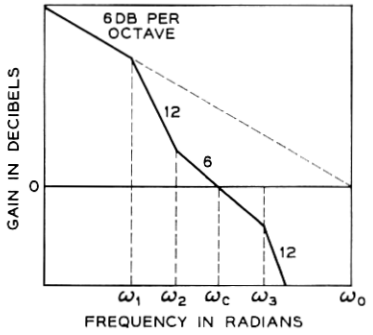

Constants

	Range (miles)			
	400–800	800–1700	1700–3500	3500–7000
Scan Rate (sec/revolution)	2	3	4	6
ω_1	0.046	0.012	0.0021	0.0021
ω_2	1.5	0.76	0.31	0.31
ω_3	150	150	150	150
ω_0	200	200	200	200

Scan Radii

Step	Degrees
0	0
1	1.4
2	2.8
3	4.2

of antenna movement. During the aided mode, an angular displacement of the same handwheel generates a constant-rate signal, which represents desired rate and direction of antenna movement. Either signal (depending on the selected mode) is amplified and applied to a low-power motor. The motor, in turn, physically positions the rotor of a synchro transformer. The position of the rotor of the control transformer represents desired antenna position. A second input to the same control transformer is an electrical input to its stator, representing actual antenna position as sensed and transmitted by a synchro transmitter that is geared to the PT antenna. The output of the control transformer represents an error between the desired antenna position and the actual

antenna position. This error signal, called "error (manual or aided)" on Fig. 15, is injected into summing point 1, where it becomes the error signal in the main servo drive circuit.

5.4 *Track Digital Control and Autotrack Modes*

During either the track digital control or the autotrack mode, the control signal is generated by circuits external to the antenna positioning circuits. The track digital control signal originates in the track digital control portion of the antenna direction system, and the autotrack signal is developed within the PT tracking receiver. Each is a dc voltage representing an error in desired antenna position. The dc voltage is converted into ac voltage by the angle modulator and is inserted into summing point 1, where it becomes the error signal within the main servo drive circuit.

5.5 *Command Tracker Mode*

During the command tracker mode, a synchro link between the precision tracker and the command tracker is used to control the main servo drive circuit of the PT. A synchro transmitter within the command tracker senses the position of the command tracker antenna and transmits this information to a synchro control transformer within the PT. The output of the synchro control transformer, representing the error between the PT and command tracker antenna shafts, is injected into summing point 1 as the error signal within the main servo drive circuit.

5.6 *Remote Control Mode*

In the remote mode, the antenna can be positioned by use of a portable control unit called the "star gaze box," which is connected by cable to the antenna base. Manual controls mounted on the star gaze box enable the operator to choose two types of control: (a) He can rapidly slew the antenna by means of switches that introduce a constant error signal into the main servo drive circuit via summing point 1. The error persists as long as the slew switch is depressed. (b) He can gently position the antenna by means of a control knob that controls the rotor of a synchro control transformer mounted in the star gaze box. A second input to the same control transformer senses actual antenna position as given by a synchro transmitter geared to the antenna. Any difference between desired antenna position, as represented by the position of the manually controlled rotor of this control transformer, and actual antenna position,

as received from the synchro transmitter, generates an error, which is fed into summing point 1 and then into the main servo drive circuit. The error persists until the antenna moves to the desired position.

5.7 *Search Scan*

In order to enhance the satellite acquisition capability of the precision tracker, the PT antenna beam can be caused to search about the mean azimuth and elevation angle to which it is pointed. The search is the result of a circular motion of the PT antenna and is controlled (either manually or automatically) by the scan control circuits located in the PT control console.

The PT antenna, as mentioned above, is positioned by two independent servo systems, one for the azimuth angle and one for the elevation angle. A separate error signal within each servo system controls antenna position in each angle. Since the PT antenna is a two-axis system, simultaneous motion in both axes is necessary if a circular pattern is to be traced about the mean angle. This is achieved by the superimposing of small offset (or bias) errors onto the main error signal in each servo system. The biasing errors are developed by the rotating rotor of a resolver, which is the key component in the scan control circuits.

Both the radius and the frequency (or period) of the circular search must also be controlled. The radius is controlled by the amplitude of the bias signals applied to the two servo systems. A choice of one of four different preset radii is available to the console operator. The desired radius is selected by means of the scan step control indicator mounted on the console. The period is established by the rate of rotation of the rotor of the resolver, which depends on the scan mode of operation.

During manual scan, the period of the PT antenna circular search is controlled by the scan handwheel drive (refer to Fig. 16). Rotation of the handwheel causes a generator to produce a voltage proportional to the speed of rotation of the handwheel. This voltage is combined with velocity feedback voltage and sent to the low-power amplifier as a motor control voltage. The motor drives the rotor of resolver B_2 at a speed proportional to the original speed of handwheel rotation and thus establishes the period of circular search. The two quadrature voltages taken from the rotor of the resolver are sent to the switch assembly, where their amplitude is regulated by the radius of scan selected by the console operator.

During the automatic scan mode, the period of the PT antenna's circular search is controlled as a function of range to ensure a good probability of beacon signal detection. At short ranges, when the satellite

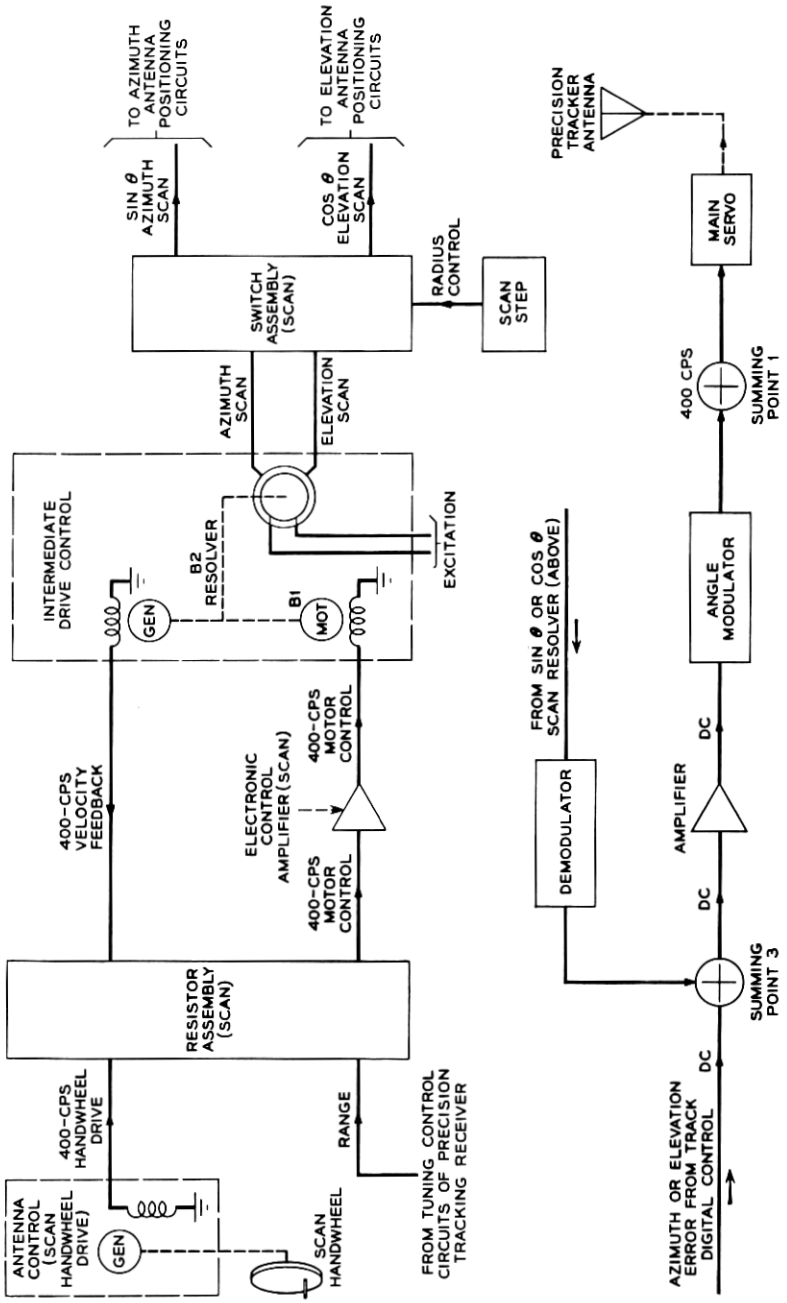

Fig. 16 — Scan control circuits.

has a high angular velocity, the antenna scans rapidly in order to search the area around the satellite. However, at longer ranges, when the angular velocity of the satellite is slower but the beacon signal strength is weaker, the antenna must search more slowly to ensure the same probability of detection.

When the track digital control mode is utilized, the orthogonal resolver rotor outputs are sent to a demodulator for conversion to a dc voltage. The automatic scan signal is then combined at summing point 3 with the track digital control error signal and converted to an ac signal in the angle modulator. This error signal is sent to the main servo drive circuit for use in positioning the antenna.

If the manual or command tracker mode has been selected, the resolver rotor output is sent directly to azimuth and elevation summing point 1.

5.8 *Data Take-Off*

The precise readout of PT azimuth and elevation angles is accomplished by 1-speed and 64-speed resolvers and analog-to-digital encoders contained in data transmitter gear boxes geared to the PT's precision data gears. These resolvers and encoders are essentially a remote extension of the track digital control and are described in another paper.[7]

VI. ACQUISITION RECEIVER

6.1 *General Description*

Owing to such factors as Doppler frequency shift and satellite oscillator drift, the frequency of the beacon signals from the Telstar spacecraft may deviate by as much as ± 150 kc about the 4079.73-mc design center frequency. The acquisition receiver (bays 1, 2, 3, 4, and 6 of Fig. 8) is employed to detect the actual received frequency and to provide an analog of this frequency for initial tuning of the phase-lock tracking receiver.

The requirement of tuning to the Doppler shifting received frequency within the period of time that the narrow antenna beam is crossing the satellite demands a rapid determination of received frequency. This is accomplished with a stationary search by use of a comb filter bank conducting a parallel observation of the frequency spectrum.

In the acquisition receiver, the sum IF signal is amplified, converted to 2.15 mc, and applied to a comb filter bank. This frequency-detection circuit consists of 300 channels housed in three cabinets, 100 in each

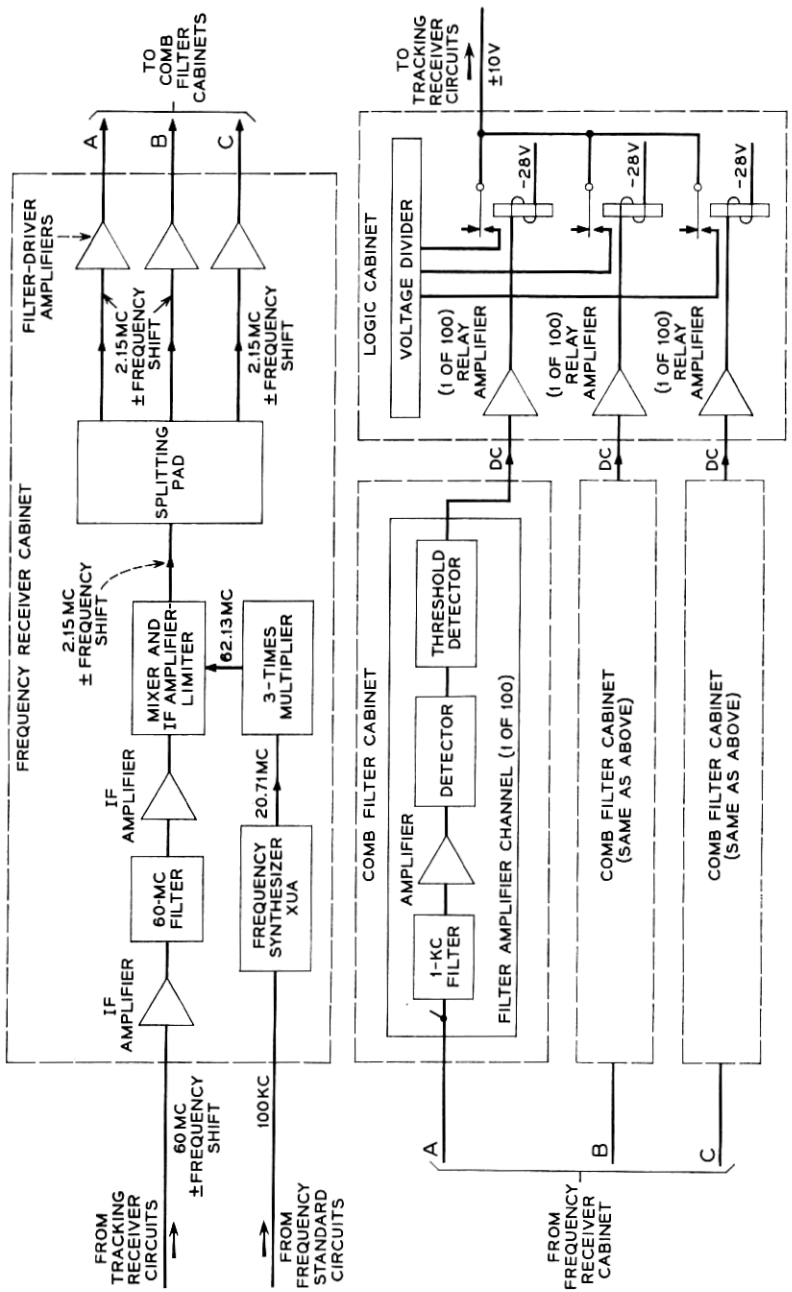

Fig. 17 — Acquisition receiver, block diagram.

cabinet. Each channel includes a narrow-band (1 kc at −1 db) crystal filter, an amplifier, a detector, a low-pass filter and a threshold circuit. All 300 detection channels are identical except that the crystal filters are cut to different center frequencies. (Filters are arranged to give a continuous coverage across the band.)

An incoming signal at the PT antenna that is within the range of 4079.73 mc ± 150 kc and is equal to or greater than noise in a 1-kc band will activate one of the comb filter channels. Overlap of the filter band-pass characteristics may cause two adjacent channels simultaneously to energize the associated threshold indicators. Normally, no more than two channels will pass a signal simultaneously. The operated channel will feed a signal to an associated relay amplifier located in the logic cabinet.

Logic circuitry determines which channel contains the received signal, disables all channels except this one and the two adjacent, and provides an analog output voltage proportional to signal frequency deviation. This voltage is supplied to the tuning control operational amplifier in the tracking receiver in order to bring a voltage-controlled crystal oscillator within the pull-in range of an automatic phase-lock loop. Once the phase-lock loop of the tracking receiver is locked, the logic input is disconnected and the frequency acquisition receiver performs no active function in the tracking. However, the acquisition circuitry is still active and can be utilized if tracking is lost. The output voltage from the acquisition receiver circuits also is sent, as an indication of received frequency, to the autotrack equipment.

6.2 *59.98-mc Amplification and Conversion*

Fig. 17 is a block diagram of the acquisition receiver. The acquisition receiver accepts 59.98-mc intermediate frequency signals and noise from the tracking receiver circuits. The two 59.98-mc IF amplifiers amplify the IF signal and noise from the sum IF amplifier in the tracking receiver circuit. The 59.98-mc narrow-band filter band limits noise to prevent overloading of the second IF amplifier.

The frequency synthesizer, synchronized to the 100-kc frequency standard, produces a signal of 20.71 mc. This signal is tripled by the 3× multiplier, which feeds a 62.13-mc signal to the mixer. The mixer produces a nominal frequency difference signal of 2.15 mc. Because of the Doppler shift in the beacon signal, the 2.15-mc signal will shift by a like amount. However, this shift will not exceed ±150 kc, which defines the limits of the comb filters.

TABLE VIII — ACQUISITION RECEIVER LEVELS

Unit	Gain (db)	Nominal Bandwidth (mc)	Minimum Signal Level (dbm)
Parametric amplifier	+18	20	−139
Mixer preamplifier	+25	8	−119
Cable	−5		−94
59.98-mc IF amplifier	+70	10	−99
59.98-mc filter with pads	−15	1	−29
59.98-mc IF amplifier	+45	10	−44
Mixer, amplifier, limiter	+50	600 kc	+1
Driver			3v rms
Comb filter			22v rms

6.3 *2.15-mc Amplification and Limiting*

The mixer output is amplified to a power level sufficient to "hard" limit the noise. In effect, the zero crossings are preserved but the peaks are clipped. The limiter output, consisting of signal plus noise, is fed to three filter driver amplifiers, which, in turn, drive the remainder of the acquisition receiver circuits.

The limiter is incorporated to establish a uniform noise threshold across the 300-kc filter bank, resulting in a constant false-alarm rate. This permits signal detection close to threshold in all channels, thus improving detection probability and simplifying logic design. After limiting, additional amplification is necessary to provide a suitable level of output to the filter driver amplifiers. A noise level set potentiometer sets the gain between the limiter and output to the comb filters. The bandwidth of each stage between the mixer and limiter is 1 mc with an over-all bandwidth of 600 kc at 3 db.

Further amplification is necessary to supply noise at the proper level for the comb filters. This is accomplished by the three filter driver amplifiers, each of which feeds the 100 filters contained in one cabinet.

6.4 *Comb Filter Channels*

Each filter-amplifier channel in the system contains a crystal filter, a two-stage amplifier, a detector, a post-detection filter, an amplifier, and a threshold circuit. The signal plus noise is filtered, amplified, and sent to the envelope detector. At this point the signal plus noise enters a 10-cps post-detection filter, after which it is amplified and compared with the threshold voltage. If its level exceeds that of the threshold voltage, the detected and amplified signal drives saturated solid-state amplifiers to provide a "signal present" dc output of −10 volts.

6.5 *Logic Circuits*

Each of the 300 comb filter channels terminates in the logic cabinet at a relay channel consisting of a transistor amplifier and relay. The relays, when operated, provide a contact closure which ties the precision voltage divider to the phase-lock loop in the track receivers of both the PT and the autotrack. In addition, the logic cabinet locks out all comb filter channels except the channel indicating a signal present and those adjacent to it. The logic circuits will follow a Doppler shifting signal and progressively lock out past adjacent channels and unlock new adjacent channels. A third feature provides a scan freeze indication to the servo scan circuits when a signal is present, in order to stop angular search.

Tests have indicated a reliable detection threshold better than -143 dbm, with a usable limit around -147 dbm, as observed during a moon bounce experiment between Holmdel and Andover.

VII. FREQUENCY STANDARD AND TEST SIGNAL

7.1 *General Description*

The frequency standard cabinet (bay 7, Fig. 8) contains circuits designed to provide stable frequencies to the precision tracker for use as local oscillator injection and testing signals. In addition, this cabinet generates the primary and secondary frequency and time references used throughout the satellite communications ground station. These references are used to adjust the station clock to the Naval Research Laboratory cesium standard at Bethesda, Maryland.

7.2 *Basic Standard*

The basic 100-kc frequency is generated in a standard master oscillator, which is in turn referenced to the VLF 18-kc Naval Station NBA. A VLF phase comparator (see Fig. 18) accepts the standard master oscillator 100-kc output and compares this frequency with an 18-kc signal received from NBA. The resultant phase difference is recorded on a strip-chart recorder. The VLF receiver also develops an audio 1-second time tick for use in the station clock. The standard master oscillator uses a highly accurate, comparator-controlled, quartz oscillator to generate a 1-mc signal. Other circuitry within the standard master oscillator utilizes the 1-mc signal in the generation of the standard 100-kc and 5-mc signals. These two signals are applied to the dis-

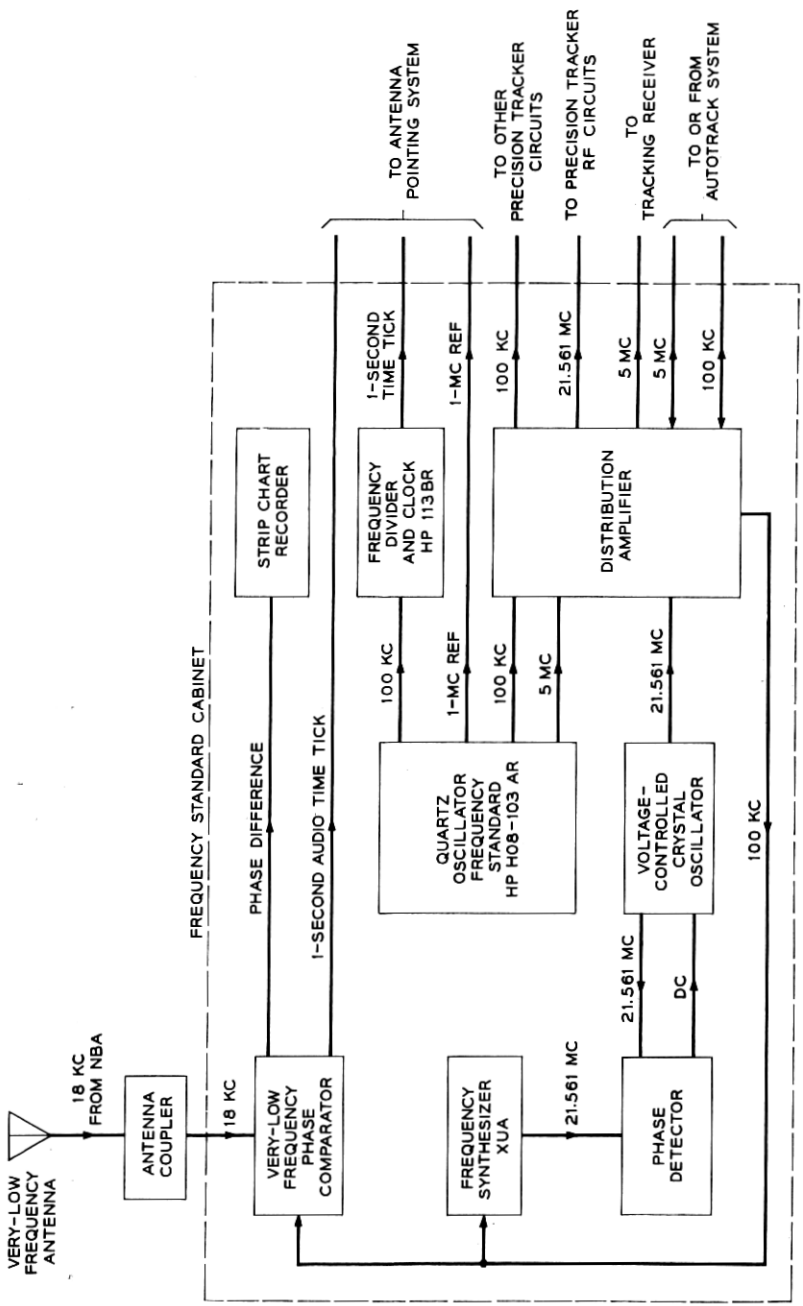

Fig. 18 — Frequency standard circuits, block diagram.

tribution amplifier, which provides amplification necessary to distribute the standard frequencies as needed throughout the PT. The 100-kc signal is also applied directly to the frequency divider and clock.

The frequency divider and clock utilizes the 100-kc signal from the standard master oscillator in the generation of a 1-second time tick. This signal is fed out of the precision tracker to the antenna pointing system along with the 1-second time tick from the VLF phase comparator for comparison purposes. An adjustment within the frequency divider and clock corrects any time deviations from NBA time. A time read-out located in the unit is also driven by the 100-kc input signal.

7.3 *Local Oscillator Signals*

A 21.561-mc signal from the frequency standard cabinet is sent to a harmonic generator, which multiplies this signal 192 times to give a 4139.71-mc local oscillator frequency for use in mixing the incoming beacon frequency (4079.73 mc), to give an IF frequency of 59.98 mc. Any variation in the initial 21.561-mc signal will be multiplied 192 times, directly affecting the stability of the track and frequency acquisition receivers. A phase-lock loop is used to minimize the variation; it consists of a frequency synthesizer, a phase detector, and a short-term, stable voltage-controlled crystal oscillator (VCXO). The frequency synthesizer derives a 21.561-mc signal from the basic standard master oscillator 100-kc output. This 21.561-mc signal is compared in the phase detector circuit with the 21.561-mc output of the VCXO.

The frequency multiplier which converts the 21.561-mc signal to 4139.71 mc is a solid-state harmonic generator consisting of two 2× multipliers, a power amplifier, a low-frequency 4× multiplier using a varactor diode in shunt configuration, a quadrupler using a self-biased diode operated in a series configuration, and a microwave tripler. The harmonic generator is designed for an input from a 50-ohm source of from 3 to 5 mw at 21.561 mc and delivers 15 mw at 4139.71 mc into a 50-ohm load.

The frequency receiver cabinet receives the 100-kc standard master oscillator signal for use in deriving the frequency acquisition receiver local oscillator injection signal. A frequency synthesizer receives the 100-kc signal and develops a 20.71-mc signal. The 20.71-mc signal is tripled to a frequency of 62.13 mc and then inserted in the local oscillator port of the frequency acquisition mixer.

Table IX shows the output levels and accuracy of each frequency discussed above.

TABLE IX — FREQUENCY GENERATION

Frequency (mc)	Cabinet	Level	Accuracy	Application
18 kc	Frequency standard	>0.1 μv	$1:10^{11}$	NBA reference
100 kc	Frequency standard	1v rms	$5\ 10^{10}$	Second LO injection frequency acquisition IF test
5	Frequency standard	1v rms		Coherent phase detection
20	Test signal	0–1v rms (0.4v nom)	Short term $1:10^{10}$ Long term $5:10^{10}$	IF test
20.71	Frequency receiver	0–1v rms (0.4v nom)		Second LO injection for frequency acquisition
21.561	Frequency standard	50 mw in 50 ohms	Long term $5:10^{10}$ Short term $1:10^{7}$	First LO injection for track receiver
60	Receiver	1–2.8v rms in 50 ohms		IF test
62.13	Frequency receiver	1–2.8v rms in 50 ohms	Long term $5:10^{10}$ Short term $1:10^{10}$	Second LO injection for frequency acquisition
4079.73	Test signal	0 dbm	±0.001%/day	RF test
4139.71	RF assembly	5 mv in 50 ohms	Long term $5:10^{10}$ Short term $1:10^{7}$	First LO injection for track receiver
Time				
1-sec audio tick	Frequency standard	1v in 600 ohms 450 msec	Same as NBA	Coarse time for station clock
1-sec tick	Frequency standard	2v in 50 ohms 200 μsec	Same as NBA	Reference time for station clock

7.4 *RF Test Signals*

The test signal cabinet contains circuits designed to provide a 4079.73-mc frequency for use as a simulated satellite beacon signal. This signal is sent through a pressurized semirigid Heliax coaxial cable to a boresight tower test horn antenna located 300 feet from the PT track mount and 600 feet from the test signal cabinet. A TD2 harmonic generator is used to generate the microwave CW test signal. The generator may be turned on and off locally at the test signal cabinet or remotely at the PT control console. A directional coupler (see Fig. 19) provides a sampling take-off for a power meter. This measurement is made to validate receiver sensitivity checks made by use of the test tower.

A phase-coherent 20-mc test signal is also developed in the test signal cabinet (Fig. 20). A 100-kc input from the standard master oscillator is

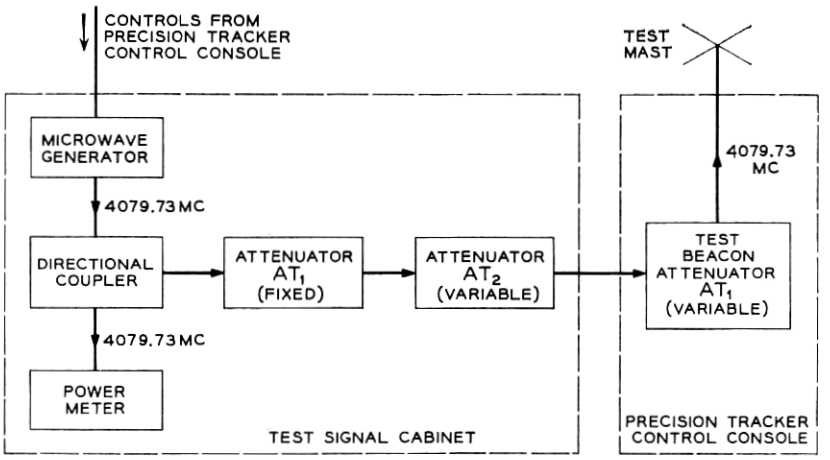

Fig. 19 — 4-kmc test signal circuits, block diagram.

multiplied to 20 mc in a frequency synthesizer. The 20-mc signal is fed to the track receiver cabinet and frequency tripled for use as a 60-mc IF test signal. A motor-driven chain drive is coupled to the frequency synthesizer to simulate Doppler shift for testing purposes.

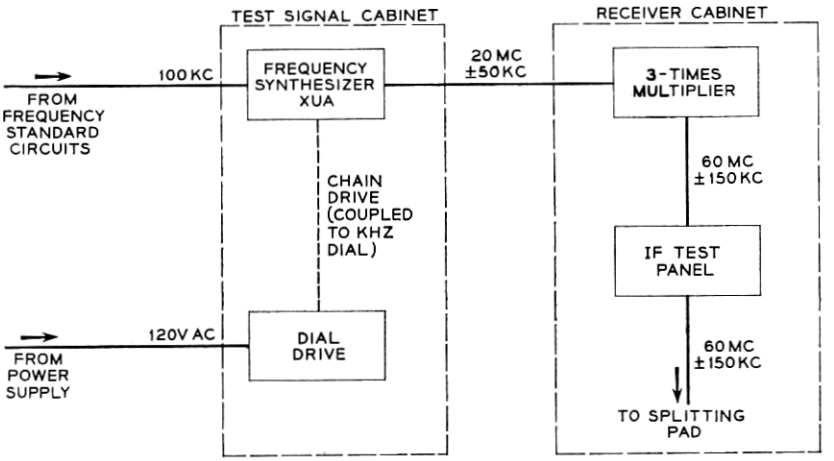

Fig. 20 — 60-mc IF test signal circuits, block diagram.

VIII. CONTROL CONSOLE

8.1 *Controls and Indicators*

Operating controls and indicators for the precision tracker are mounted on the PT control console (Fig. 21). Among the controls on the console are switches used to select mode of operation and input data source, handwheels used to point the antenna and scan the beam manually, and controls used to search in frequency. Indicators on the console include lamps showing PT and system status; meters showing azimuth error, elevation error, range, signal strength, and frequency deviation; and decimal readouts of station time and PT antenna angle data. In addition, an array of test function switching controls is located behind the upper right-hand door.

The various acquisition modes, discussed in Section V, are controlled at the console. The three operational groupings include elevation at the left, azimuth in the center, and frequency at the right. Experience has shown that only one operator, seated centrally before the azimuth position, is required. His duties are mainly to precondition the system before a pass and monitor the acquisition and tracking processes during the

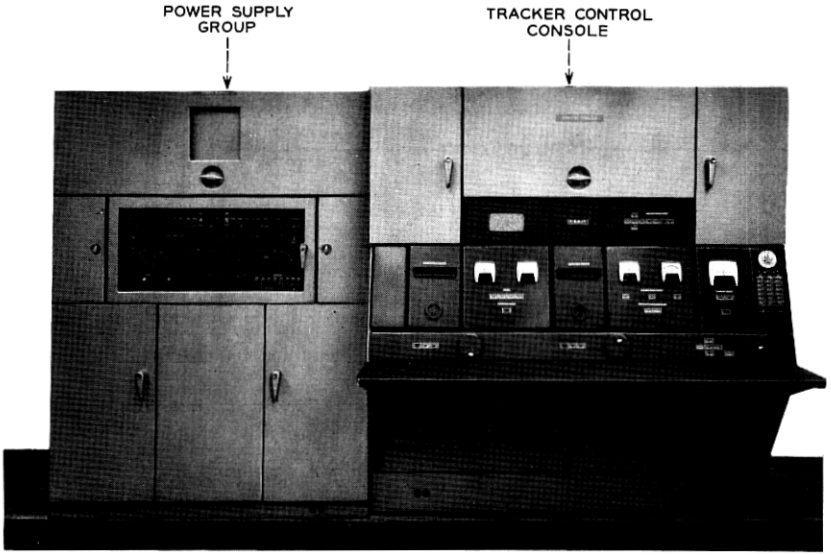

Fig. 21 — Console and power supply group.

pass. He can intervene to change modes or manually search in angle and frequency. The operator can read out Doppler shift, received signal strength, and tracking perturbations if requested by the tracking director.

8.2 *Power System*

The precision tracker uses both 120/208-volt, 400-cycle, 3-phase power and 120-volt, 60-cycle, single-phase power in its operation. The 400-cycle power is fed directly to the PT power control cabinet (Fig. 22) for operation of power supplies in the cabinet and for distribution to the antenna positioning circuits. "Technical" 60-cycle power is distributed from a wall panel to the acquisition and tracking receivers and to the frequency standard, VLF, and test circuits. "Utility" 60-cycle power is distributed from another wall panel to outlets in the PT equipment cabinets.

IX. ANTENNA ASSEMBLY AND TOWER

The physical specifications associated with the major structures of the precision tracker system are listed below.

(1) Antenna Assembly	
Weight	7000 pounds
Height, jack pads to elevation axis	11 feet 9 inches
Torques:	
Overturning, 60-mph wind	8700 ft-lbs
Overturning, 120-mph wind	27,200 ft-lbs
Rotational in horizontal plane	650 ft-lbs max.
(2) Antenna Tower (Fig. 22)	
Concrete with hexagonal cross section	
Height, base to elevation axis	35 feet 8 inches
Twist at 650 ft-lbs torque	0.05 milliradian max.
Sway	0.05 milliradian max.
Settling:	
Per day	0.03 milliradian max.
Limit	45 milliradians, total
(3) Test Tower	
Distance from antenna tower	300 feet
Height	60 feet
Twist in 40-mph wind	± 3 minutes max.
Sway at top in 40-mph wind	± 0.06 inch max.

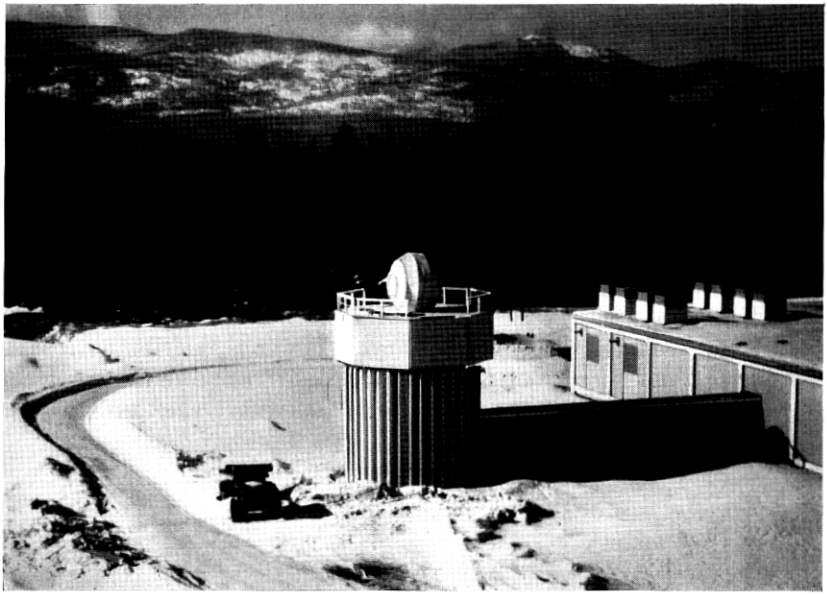

Fig. 22 — PT antenna tower at Andover, Maine, radome deflated.

X. TEST DATA AND OPERATING EXPERIENCE

10.1 *Operating Noise Temperature*

The input noise power from all sources including antenna, sky, and radome as measured by the CW signal substitution method is −138 dbm at an elevation of 0 degree. The measurement was made in the 3-kc bandwidth of the tracking receiver's sum channel to an accuracy of 0.9 db. The receiver noise figure, which was also measured, was found to be 3.1 db corresponding to a noise temperature of 315°K. The total effective noise temperature, for an elevation angle of 10 degrees, is estimated as follows:

Sky	13.5°K
Side lobes	2.5°K
Radome	9°K
Input temperature of receiver including comparator and fittings	315°K
Total at 10° elevation	340°K

The variation in system noise with elevation angle was also meas-

ured. This is shown in Fig. 7. The slight increase at the zenith is typical of a daytime measurement and is caused by coupling to the sun. Similar measurements made at night reveal the expected minimum at the zenith. −139 dbm is taken as a receiver signal power reference for a 0-db signal-to-noise ratio in the 3-kc bandwidth of the sum channel.

A careful measurement was made of the degradation in sensitivity with the parametric amplifiers bypassed. The increase in effective system input noise was measured as 7 db. This figure was obtained by relation of the signal-to-noise ratios obtained in each condition for the same fixed input signal level.

10.2 *Received Signal Levels*

Received signal levels for six typical passes of the Telstar spacecraft are plotted in Fig. 23. In this figure, signal level is plotted as a function of slant range, a technique adopted during the first days of tracking to enable on-the-spot checks of beacon transmitter and PT performance. The reference line is plotted as a 6-db per octave slope to account for variation in path loss with range; it assumes +17 dbm radiated beacon power and a truly isotropic antenna on the satellite. The 0-db SNR is based on the −139 dbm effective input noise power of the PT. The data were plotted point by point during each pass, taking slant range from the mission printout at the time of measurement; SNR was read from the calibrated signal strength meter on the PT console.

The measured SNR may generally be expected to fall below the reference slope. Variations in communications power from none to maximum may cause the beacon power to vary from the nominal +17 dbm to +15 dbm with full power in the communication channel. These variations appear on the measured SNR curves as the minor fluctuations departing from the generally smooth curve; they were correlated in time with the changing power levels indicated by the accompanying communication experiments during the first several passes.

The general trend of departure from the 6 db/octave slope is a function of the satellite's antenna pattern and the changing spin angle. Reference to the spin angle predictions and the antenna pattern showed a correlation within 1 db.

10.3 *Tracking Jitter*

The variation of angle tracking jitter with signal-to-noise ratio is shown in Fig. 24. The test consisted of tracking the RF test signal from the boresight tower. The data shown are for the azimuth coordi-

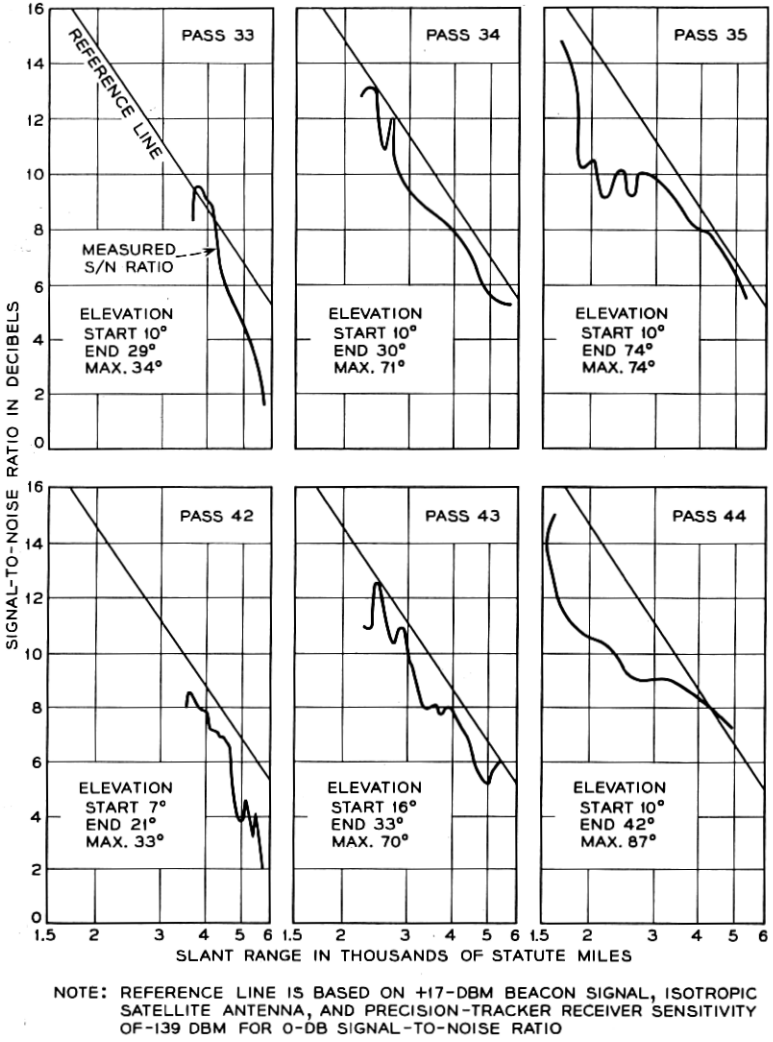

Fig. 23 — Received signal levels.

nate; the elevation data agreed more closely with the theoretical performance.[8]

10.4 *Phase Jitter and Frequency Measurements*

The coherence time, or phase jitter, of the beacon signal is a critical parameter in the performance of the PT and the autotrack. The phase-

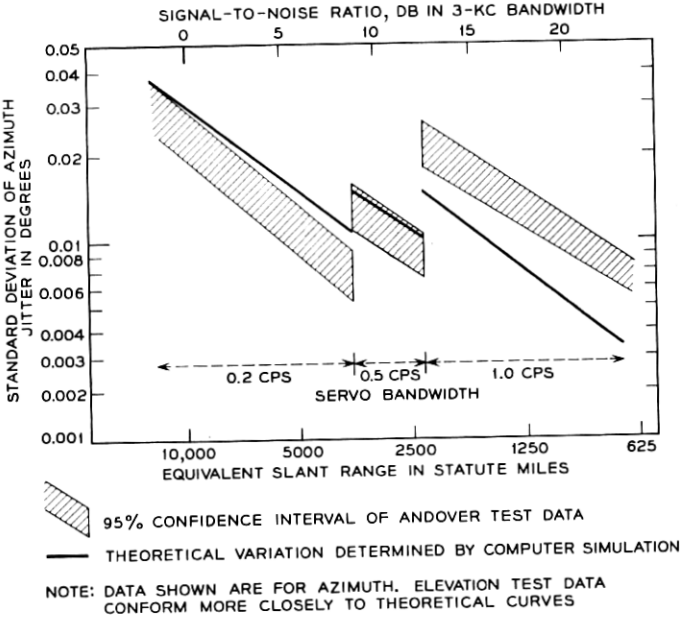

Fig. 24 — Angle tracking jitter.

lock loop of the PT tracking receiver has been employed to measure this parameter of different beacon sources, including models of the Relay and Telstar satellites and the Holmdel, N.J., 4079.73-mc transmitter employed to illuminate Echo I for tracking tests. In all cases, the jitter of the beacon signals made a negligible contribution to the total jitter in the phase-lock loop.

XI. ACKNOWLEDGMENTS

Credit for the successful completion of the precision tracker is due to many individuals and organizations. The staff of Wheeler Laboratories, Incorporated, designed and tested the Cassegrainian twist-reflector antenna and the microwave comparator/feedhorn assembly and provided valuable consultation throughout the program. Itek Corporation designed and produced the 300-channel comb filter. Mr. K. B. Woodard and members of his group were responsible for the mechanical design of the antenna, the RF assembly, and data units, and for testing the mechanical accuracy of the antenna assembly. Messrs. W. L. Nelson, R. W. Hatch, R. Lowell, L. H. Enloe, and R. H. Turrin made important

analysis and design contributions in the development of the phase-lock loop and coherent angle-error detectors.

REFERENCES

1. Davis, C. G., Hutchison, P. T., Witt, F. J., and Maunsell, H. I., The Spacecraft Communications Repeater, B.S.T.J., this issue, p. 831.
2. Githens, J. A., Kelly, H. P., Lozier, J. C., and Lundstrom, A. A., Antenna Pointing System: Organization and Performance, B.S.T.J., this issue, p. 1213.
3. Hannan, P. W., Optimum Feeds for All Three Modes of a Monopulse Antenna I and II, Trans., I.R.E., **AP-9,** 1961.
4. Rhodes, D. R., *Introduction to Monopulse*, McGraw-Hill, New York, 1959.
5. Reed, E. D., Diode Parametric Amplifiers — Principles and Experiments, Semiconductor Products, **4,** Jan., 1961, pp. 25–30, and Feb., 1961, pp. 35–42.
6. Nelson, W. L., Analysis of the Angle-Error Detection System for Automatic Tracking of *Telstar* Satellites, to be published.
7. Githens, J. A., and Peters, T. R., Digital Equipment for the Antenna Pointing System, B.S.T.J., this issue, p. 1223.
8. Ball, W. H. W., Analysis and Digital Simulation of the *Telstar* Precision Tracker, Paper No. CP-63-368, presented at the IEEE Winter General Meeting, New York, 1963.